The Interplay between Carbon Availability and Growth in Different Zones of the Growing Maize Leaf[1][OPEN]

Angelika Czedik-Eysenberg, Stéphanie Arrivault, Marc A. Lohse, Regina Feil, Nicole Krohn, Beatrice Encke, Adriano Nunes-Nesi, Alisdair R. Fernie, John E. Lunn, Ronan Sulpice, and Mark Stitt*

Gregor-Mendel-Institute of Molecular Plant Biology, 1030 Vienna, Austria (A.C.-E.); Max Planck Institute of Molecular Plant Physiology, 14476 Potsdam, Germany (S.A., R.F., N.K., B.E., A.R.F., J.E.L., M.S.); Targenomix GmbH, 14476 Potsdam, Germany (M.A.L.); Departamento de Biologia Vegetal, Universidade Federal de Viçosa, 36570-900 Viçosa, Minas Gerais State, Brasil (A.N.-N.); and Plant Systems Biology Lab, Plant AgriBiosciences, C314 Aras de Brun, National University of Ireland, Galway, Ireland (R.S.)

ORCID IDs: 0000-0002-7027-802X (A.C.-E.); 0000-0001-8533-3004 (J.E.L.); 0000-0002-6113-9570 (R.S.).

Plants assimilate carbon in their photosynthetic tissues in the light. However, carbon is required during the night and in nonphotosynthetic organs. It is therefore essential that plants manage their carbon resources spatially and temporally and coordinate growth with carbon availability. In growing maize (*Zea mays*) leaf blades, a defined developmental gradient facilitates analyses in the cell division, elongation, and mature zones. We investigated the responses of the metabolome and transcriptome and polysome loading, as a qualitative proxy for protein synthesis, at dusk, dawn, and 6, 14, and 24 h into an extended night, and tracked whole-leaf elongation over this time course. Starch and sugars are depleted by dawn in the mature zone, but only after an extension of the night in the elongation and division zones. Sucrose (Suc) recovers partially between 14 and 24 h into the extended night in the growth zones, but not the mature zone. The global metabolome and transcriptome track these zone-specific changes in Suc. Leaf elongation and polysome loading in the growth zones also remain high at dawn, decrease between 6 and 14 h into the extended night, and then partially recover, indicating that growth processes are determined by local carbon status. The level of Suc-signaling metabolite trehalose-6-phosphate, and the trehalose-6-phosphate:Suc ratio are much higher in growth than mature zones at dusk and dawn but fall in the extended night. Candidate genes were identified by searching for transcripts that show characteristic temporal response patterns or contrasting responses to carbon starvation in growth and mature zones.

Plants experience a daily alternation of light and darkness. While growth in the light can use newly fixed carbon (C), growth at night depends on reserves that are built up in preceding light periods (Smith and Stitt, 2007). Many plants accumulate part of the newly fixed photosynthate as starch in their leaves in the light, and remobilize this starch to support metabolism and growth at night (Zeeman et al., 2010; Weise et al., 2011). In fast growing plants, starch is almost, but not completely, exhausted at dawn (Kalt-Torres et al., 1987; Gibon et al., 2004b; Graf et al., 2010; Sulpice et al., 2014). This maximizes growth by ensuring that almost all the photosynthetically fixed C is immediately invested, while avoiding detrimental periods of C starvation at the end of the night (Graf and Smith, 2011; Stitt and Zeeman, 2012). C starvation during the night leads to an inhibition of growth, which is not immediately reversed in the next photoperiod (Gibon et al., 2004a; Yazdanbakhsh et al., 2011). It also activates catabolic processes, resulting in a wasteful cycle of biomass synthesis and degradation at different times in the 24 h cycle (Brouquisse et al., 1992, 1998; Devaux et al., 2003; Thimm et al., 2004; Usadel et al., 2008; Izumi et al., 2010; Honig et al., 2012; Ishihara et al., 2015).

Starch turnover is adjusted to changes in photoperiod, irradiance, and CO_2 concentration such that when less photosynthate is available per 24 h cycle, proportionately more photosynthate is invested into starch and the rate of starch degradation is decreased (for review, see Smith and Stitt, 2007; see also Gibon et al., 2009; Sulpice et al., 2014). Starch is degraded at an almost constant rate throughout the night, and this rate varies such that starch is almost but not entirely exhausted at dawn. The timing of starch degradation requires the circadian clock (Graf et al., 2010; Graf and Smith, 2011; Scialdone et al., 2013). Suc levels in Arabidopsis (*Arabidopsis thaliana*) rosettes are fairly constant for much of the night in a given photoperiod (Martins et al., 2013; Pal et al., 2013; Sulpice et al., 2014) but decrease as the photoperiod is shortened, mirroring the lower rate of starch degradation (Sulpice et al., 2014).

[1] This work was supported by the Max-Planck Society.

* Address correspondence to mstitt@mpimp-golm.mpg.de.

The author responsible for distribution of materials integral to the findings presented in this article in accordance with the policy described in the Instructions for Authors (www.plantphysiol.org) is: Mark Stitt (mstitt@mpimp-golm.mpg.de).

M.S. and R.S. designed the research; A.C.-E., S.A., N.K., B.E., R.F., and A.N.-N. conducted research; M.A.L. contributed computational tools and valuable statistical advice; A.C.-E. analyzed data; A.R.F. and J.E.L. gave support in experiment planning and writing the paper; A.C.-E. and M.S. wrote the manuscript.

[OPEN] Articles can be viewed without a subscription.

www.plantphysiol.org/cgi/doi/10.1104/pp.16.00994

The maintenance of a balanced C budget also requires regulation of the rate of C utilization, in particular for growth. By setting the rate of starch degradation, the clock regulates the rate of Suc formation at night. This may allow indirect regulation of growth. Protein synthesis represents a major component of cellular growth (Warner, 1999; Rudra and Warner, 2004). Polysome loading provides a qualitative proxy for protein synthesis. There is a robust correlation between Suc content and polysome loading, in particular loading of cytosolic ribosomes in polysomes, across a wide range of conditions (Pal et al., 2013; Sulpice et al., 2014).

A growing number of signaling pathways have the potential to coordinate growth with the C supply (Ingram and Waites, 2006; Smeekens et al., 2010; Lastdrager et al., 2014; Sheen, 2014) including the target of rapamycin complex (Deprost et al., 2007; Xiong et al., 2013; Xiong and Sheen, 2014), SNF-related kinase1 (SnRK1; Baena-González et al., 2007; Halford and Hey, 2009; Dong et al., 2012), the C/S1-bZIP transcription factor network (Wiese et al., 2005; Kang et al., 2010; Ma et al., 2011; Thalor et al., 2012), HEXOKINASE1 (HXK1; Jang and Sheen, 1994; Moore et al., 2003; Cho et al., 2006; Granot et al., 2013; Kim et al., 2013), and the Suc-signal trehalose-6-phosphate (T6P; Paul et al., 2008; Smeekens et al., 2010; Lastdrager et al., 2014; Lunn et al., 2014). A bidirectional relationship between T6P and Suc levels has been proposed, in which high Suc levels lead to an increase in T6P and, in turn, high T6P promotes Suc utilization, leading to a reduction in Suc level (Lunn et al., 2014; Yadav et al., 2014). Arabidopsis plants overexpressing the T6P-synthesizing enzyme trehalose-phosphate synthase or the T6P-degrading enzyme trehalose-phosphate phosphatase show pronounced opposite phenotypes with alterations in growth and development (Schluepmann et al., 2003). T6P post-translationally activates nitrate assimilation, and organic acid and amino acid synthesis (Figueroa et al., 2016) induces genes required for anabolic pathways in Arabidopsis (Zhang et al., 2009) and promotes developmental transitions such as flowering (Wahl et al., 2013). It has been proposed that T6P may in part act by inhibiting SnRK1 (Zhang et al., 2009; O'Hara et al., 2013; Lawlor and Paul, 2014).

Spatially resolved analyses are needed to understand the relationship between C availability and growth. Growth includes cell division and cell expansion, and both require the production of structural components like protein and cell wall polysaccharides (Stitt, 2013). Much recent research on the relation between C availability and growth was carried out using Arabidopsis rosettes. This reference dicot species has excellent genome and genetic resources and the logistic advantages of small size and a short life cycle. However, for spatially resolved analyses of metabolism and growth, the growing maize (*Zea mays*) leaf blade has two major advantages: First, expansion growth can be monitored at high temporal resolution as the increase in leaf length (Ben-Haj-Salah and Tardieu, 1995; Tang and Boyer, 2008; Poiré et al., 2010). In Arabidopsis, highly resolved measurement of growth rates is difficult due to the small size of growing leaves and because the roundish shape of dicotyledonous leaves requires measurement of changes in area (Wiese et al., 2007; Apelt et al., 2015). Second, and crucially, it is easier to separate and analyze growing and mature leaf tissues: For a given cell line, a phase of cell division is followed by phases of cell expansion and maturation (Sylvester et al., 1990; Andriankaja et al., 2012; Gonzalez et al., 2012). The growing monocot leaf blade has a well-defined developmental gradient, with a cell division zone at the base directly above the preligula band, followed by zones of cell elongation and maturation, with mature photosynthetic tissue at the leaf tip (Sylvester et al., 1990; Meiri et al., 1992; Ben-Haj-Salah and Tardieu, 1995). Moreover, compared to other linearly organized organs such as Arabidopsis roots, maize leaves have the advantage of size making it feasible to collect sufficient material from individual developmental zones for omics studies (Avramova et al., 2015b).

Recent studies examined the transcriptome (Li et al., 2010; Wang et al., 2014), proteome (Majeran et al., 2010), phosphoproteome (Facette et al., 2013), and metabolome (Pick et al., 2011; Wang et al., 2014) along the maize leaf developmental gradient. They found considerable differences between the different growth zones and mature tissue. Nelissen et al. (2012) studied the distribution of major phytohormones within the growth zones of maize leaves and found that gibberellic acid reaches a peak level in the transition zone between cell division and expansion zones and plays a significant role in controlling the size of the cell division zone and, by this way, leaf elongation rate. Another recent study of drought effects on cellular growth processes in the maize leaf growth zones (Avramova et al., 2015a) uncovered a role for local antioxidant capacity in promoting cell division, which is up-regulated during drought, partly counteracting the inhibition of cell division due to down-regulation of cell cycle genes. These two studies underline that regulatory processes that affect growth occur locally in the growth zones.

The following experiments investigate the response of central metabolism and gene expression to a decrease in the C supply during the night and an extended night treatment in the growing maize leaf, using a similar experimental design to that previously used for Arabidopsis (Usadel et al., 2008). We analyze the response of metabolism and gene expression in leaf zones that are undergoing cell division or cell expansion and in mature leaf tissue and link them to two growth traits; the overall rate of leaf elongation and polysome loading as a proxy for protein synthesis.

RESULTS

Examination of Four Developmentally Distinct Regions of the Growing Maize Leaf Blade over a C Starvation Time Course

We harvested leaf 9 from approximately 3.5-week-old maize plants. This is about 3 d after leaf 9 emerges from the whirl. The leaf sheath, which is located below the ligula, was <4 mm long and was not yet significantly

expanding, the leaf blade was undergoing rapid elongation, and the leaf tip was green and photosynthetically active (Fig. 1A). We took samples from four distinct regions along the leaf developmental gradient: Regions R1 to R3 were taken from the immature base of the leaf blade, 0 to 1.5 cm (R1), 1.5 to 3 cm (R2), and 3 to 4.5 cm (R3) above the preligula band. Based on earlier studies (Meiri et al., 1992; Ben-Haj-Salah and Tardieu, 1995) these samples should correspond to the cell division zone, the transition zone between cell division and elongation, and a basal section of the cell elongation zone, respectively. R4 corresponds to part of the mature leaf. Samples were taken from each zone at five time points: just before the end of the light period (ED), and just before the end of the night (EN) of the 14 h light/10 h dark diurnal cycle, and after a 6, 14, and 24 h extension of the night (6hExN, 14hExN, and 24hExN, respectively). The harvests at ED and EN provide information about the metabolic state and available reserves at the end of the day and at the end of the night, and the successive harvests during the ExN reveal how maize leaves respond to further C depletion. For each time point, leaf zone, and experimental repetition, three biological replicates were taken, each consisting of material from five plants. The five sequential sampling times, ED, EN, 6hExN, 14hExN, and 24hExN, will be referred to as the "C depletion time course."

We used two approaches to confirm the assumed identity of the sampled zones. First, we determined the extent of nucleus duplication by flow cytometry, using samples taken 4 h into the light period. This provides information about the ratio of duplicated nuclei (i.e. nuclei in the G2 phase of cell cycle) compared to nonduplicated (G1) nuclei (Dolezel et al., 2007). The highest frequency of duplicated nuclei is found in R1, in line with its specification as the "cell division" zone (Supplemental Fig. S1A). The nucleus duplication rate is intermediate in R2 and significantly (*t* test; *P* value: 0.003) lower in R3, the presumed "elongation zone" sample. However, we also find a lower but nonzero frequency of duplicated nuclei in the mature leaf tissue (R4), which is probably due to endoreduplication (see Ben-Haj-Salah and Tardieu, 1995). Second, we determined the location of the cell division zone by microscopic analysis, using methodology based on Rymen et al. (2010) and Nelissen et al. (2013): Nuclei in the epidermal cell layer were stained by 4′,6-diaminophenylindole and the ratio of dividing nuclei to all nuclei was determined at 3 mm increments over the base of the leaf blade (Supplemental Fig. S1B, indicated in red). A polynomial function fitted through the data points indicates the cell division zone from the ligule up to approximately 2.8 cm above with maximal cell division rate approximately 1.5 cm above the ligule, which corresponds to the peak in nucleus duplication rate (Supplemental Fig. S1A). We also used microscopy to obtain a cell length profile over the first 10 cm of the growing maize leaf blade, from which we derived the extent of the cell elongation zone (Supplemental Fig. S1B). We observe that cells within the first cm above the ligule are longer than in the second cm above the ligule, so that the minimal cell length corresponds to the peak in cell division rate at approximately 1.5 cm into the leaf. Cell elongation starts beyond this point, at about 1.65 cm above the ligule, and final cell length is reached about 9.5 cm above the ligule. In summary, this microscopic analysis confirms that the first sampled region (R1) contains tissue where cell division is occurring but not yet cell elongation, the second leaf region (R2) covers a transitory zone in which division and elongation is occurring, and from region R3 onwards, cell division has ceased and cells are only elongating. Further and independent confirmation of the identities of the sampled leaf regions is provided later, based on analysis of gene expression profiles.

Metabolite Profiling in Four Leaf Zones during the C Depletion Time Course

We profiled 64 metabolic traits using photometric/colorimetric assays (Gibon et al., 2004a), gas chromatography-mass spectrometry (GC-MS; Tohge et al., 2011) and liquid chromatography-mass spectrometry triple quad analysis (Lunn et al., 2006). The profiled traits included starch, sugars, sugar phosphates, organic acids, and amino acids, as well as important metabolic precursors and degradation products such as shikimate and urea and the Sucsignal T6P. Our dataset also includes maximum activity measurements (i.e. capacity) for 11 enzymes in central metabolism. The data and individual figures for each trait are provided in Supplemental Datafiles S1 and S2.

We used principal component analysis (PCA) to provide an overview of the metabolic response (Fig. 1B). Since metabolic traits have different distributions of absolute values, measurement values for each trait were converted to z-scores before analysis (see "Materials and Methods" for more details). PC1 captures about 32% of variation and separates the four leaf zones. The mature leaf region is strongly separated, and the three growth zones lie closer together, with the elongation zone slightly closer to the mature leaf than the other two zones. PC2 captures about 27% of variation and separates samples along the C-depletion time course. Whereas in the mature leaf zone EN is clearly separated from ED, in the three growth zones EN is still close to ED.

In a second global analysis, we compared the extent to which metabolic traits change in each zone, relative to their value at ED. To do this, we calculated for each zone the change between ED and each of the other time points for each metabolic trait, using z-score-converted values. The changes were then averaged across all metabolic traits, after converting negative to positive values (Fig. 1C; see "Materials and Methods" for formula). We term this the "mean metabolic change relative to ED." The mean metabolic change relative to ED is significantly larger in the mature leaf region than in the growth zones at all times except 14hExN (*P* values: < 0.001). It also changes earlier in the mature leaf zone; in the mature zone, there is already a large difference between ED and

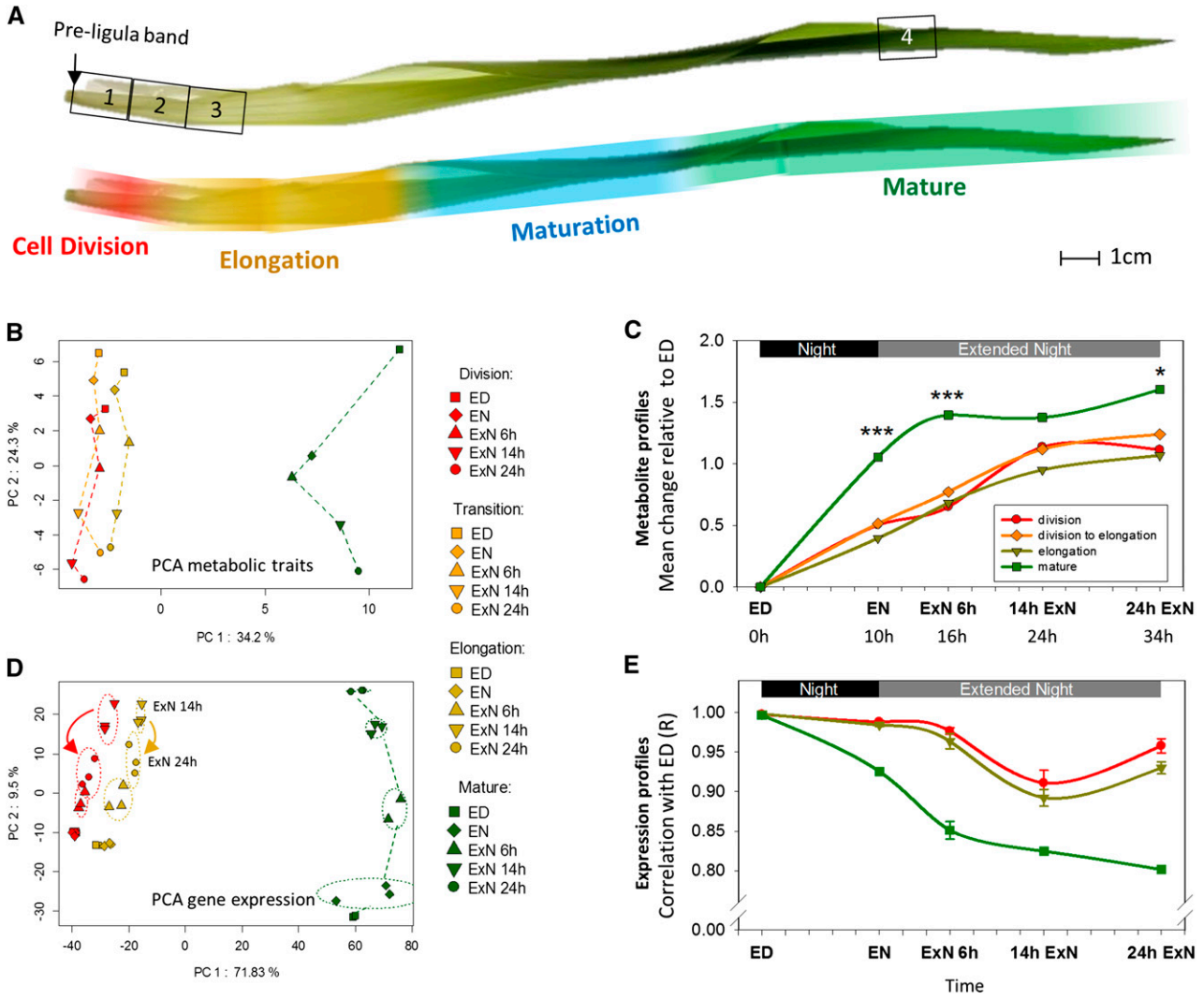

Figure 1. Metabolic and gene expression profiles differ considerably between growth zones and mature tissue of the growing maize leaf blade and show a differential carbon starvation response. A, The leaf blade developmental gradient of leaf 9. Top, Numbers 1 to 4 indicate the positions where samples were taken. 1, Division; 2, division to elongation/transition; 3, elongation; 4, mature. Bottom, The approximate positions of cell division zone, elongation zone, differentiation zone, and mature leaf tissue along the leaf developmental gradient are indicated by false color overlays. Data to support this are provided in Supplemental Figure S1. B and D, PCA of metabolic profiles (B) and expression profiles (D) from samples taken from the indicated leaf zones over a carbon starvation time course. Expression profiling was only performed for zones 1, 3, and 4. Averages values from typically three replicates for 75 metabolic traits were z-score transformed before analysis (see "Materials and Methods"). Affymetrix gene expression data were filtered before analysis (see text for details), and typically three replicates for each region and time point were plotted individually. PC, Principal component. C and E, The overall pattern of change in metabolite (C) and expression (E) profiles over the time course in the zones. C, To calculate mean metabolic change relative to ED, we first transformed values for each metabolic trait within each leaf region to z-scores. We then calculated for each metabolic trait and leaf region the difference between the z-score transformed trait value at a given time point to the value at ED. These differences were averaged over all traits for each time point and leaf region, with negative difference values having been converted to positive (please see "Materials and Methods" for more details). Error bars are omitted for clarity. Stars indicate a significant difference between the mean metabolic change in the mature tissue and each of the growth zone samples at the given time point. E, To quantify the change of expression profiles over the time course, the list of expression values measured for a given leaf zone and time point was correlated against the list of expression values measured in the same zone at ED. This calculation was performed for all permutations of replicate Affymetrix arrays. Error bars: SD between correlation values obtained in all permutations. ED, End of day, EN, end of night, ExN 6h/14h/24h, extension of the night by 6 h/14 h/24 h; *x* axis ticks indicate 2 h intervals. In C, the time in hours since start of the experiment (=ED) is indicted below the time points; ***P value < 0.001; *P value < 0.05.

EN, and the average change plateaus by 6hExN, whereas in the growth zones, the change between ED and EN is much less pronounced and the maximum response is not reached until 14hExN. In summary, first, metabolism differs markedly between growth and mature zones and, second, the metabolic response during the C depletion time course is less pronounced and delayed in the growth zones compared to mature tissue.

Clustering of Metabolites Reveals Differences in the C Starvation Response between Leaf Zones

We preformed hierarchical clustering to investigate how individual metabolic traits change during the C depletion time course in the different leaf zones (Fig. 2). The clustering used z-score transformed values. In some cases, the same metabolic trait was determined by two methods (e.g. 2-oxoglutarate was determined by GC-MS and liquid chromatography-mass spectrometry triple quad analysis). In such cases, the values from both measurements were retained to provide a quality control. Generally, the parallel measurements cluster together.

Hierarchical clustering separated the metabolic traits into five groups. Group 1 contains traits that are low in the growth zones, high in mature tissue and show, compared to this development gradient, little response to C depletion. This group includes chlorophyll and photosynthetic and C4 pathway enzymes. It also includes the intermediate phospho*enol*pyruvate, although this metabolite did decline between ED and 6hExN and rose at the end of the dark treatment in mature leaf tissue. The maintenance of the photosynthetic machinery in the extended night resembles the response in Arabidopsis (Gibon et al., 2004b; Usadel et al., 2009). Group 2 contains traits that at ED are low in the growth zones and high in mature tissue. These traits remain low in the growth zones during C depletion. In mature tissue, they decrease strongly between ED and EN and remain low in the extended night. These include the Calvin-Benson cycle intermediates 3-phosphoglycerate and Fru 1-6-bisphosphate, the photorespiratory metabolite glycerate, and the C4 metabolic shuttle intermediate pyruvate.

Group 3 contains traits that are higher in the growth zones than in mature tissue. Many traits in this group decrease during the C-depletion time course, especially in the growth zones. Group 3 includes T6P, the central glycolytic enzyme phosphofructokinase, as well as hexose phosphates and succinate, which indicates that glycolysis and the TCA cycle may operate at higher capacities in the growth zones. The C4 metabolic intermediate malate also falls into this group. Malate is higher in the transition and elongation zones than in mature tissue throughout the time course (Supplemental Datafile S3). This is unexpected, as most other C4 metabolites and enzymes are higher in the mature tissue (group 1; see "Discussion"). Group 3 also contains protein. Protein content in the growth zones was high at ED and EN and decreased significantly at 24hExN, whereas there was no significant change in protein content in the mature region (Supplemental Datafile S1; Supplemental Fig. S2B).

Group 4 contains metabolic traits that increase toward the end of the C depletion time course. It contains several amino acids (see Supplemental Datafile S2 for individual displays). While nitrogen-rich amino acids (Asn, Lys, Arg) increase mainly in the growth zones, aromatic amino acids (Phe, Trp) increase most strongly in mature tissue. Most amino acids plateau between 14hExN and 24hExN; however, Asn continues to rise until 24hExN. Some traits in group 4 increase in the growth zones but not in mature tissue; this includes glycerol-3-P and Glu dehydrogenase (Glu-DH). Glycerol 3-P is presumably formed during lipid catabolism. Glu-DH is involved in amino acid catabolism, deaminating Glu to produce the TCA-cycle intermediate 2-oxoglutarate. While Glu-DH shows constant activity in the mature tissue, it is induced during the ExN in the growth zones (Supplemental Fig. S7B). The responses in group 4 indicate that protein and amino acid degradation are induced to remobilize C, in line with studies in maize roots (Brouquisse et al., 1998) and Arabidopsis seedlings and rosettes (Thimm et al., 2004; Osuna et al., 2007; Usadel et al., 2008).

Group 5 comprises traits that are high at ED and decrease during the C-depletion time course in all zones. This group contains starch, Suc, Glc, and Fru (Fig. 3). It also includes intermediates in biosynthesis pathways, including the starch precursor ADP-Glc, the Suc precursor Suc-6-phosphate, the cell wall component precursor myoinositol, the aromatic amino acid biosynthesis pathway intermediate shikimate, as well as 2-oxoglutarate, the acceptor for NH_3 in the GOGAT pathway (Supplemental Fig. S7D; see below). While all leaf zones show the same general response, important differences can be discerned. Whereas in mature tissue carbohydrates are almost depleted by EN, in growth zones they show only a small decrease during the night and are not depleted until 6 to 14 h into ExN (Fig. 3). Suc shows a significant partial recovery at 24hExN in the growth zones, where it recovered to over half the EN value ($P = 0.011$, 0.026, and 0.009 in R1, R2, and R3, respectively; Fig. 3A). This partial recovery was confined to the growth zones and was largely restricted to Suc, with no recovery of starch or reducing sugars (Fig. 3). Interestingly, at ED, Suc in the growth zones was 60%, 40%, and 5% lower (in the elongation, transition, and division zone than in mature tissue; Fig. 3A). This decrease of Suc in growth compared to mature zones would be even larger if Suc were related to protein content (compare Fig. 3A and Supplemental Fig. S2).

To provide higher spatial resolution for starch, complete leaves were harvested at different times and stained with iodine (Supplemental Fig. S3). In line with

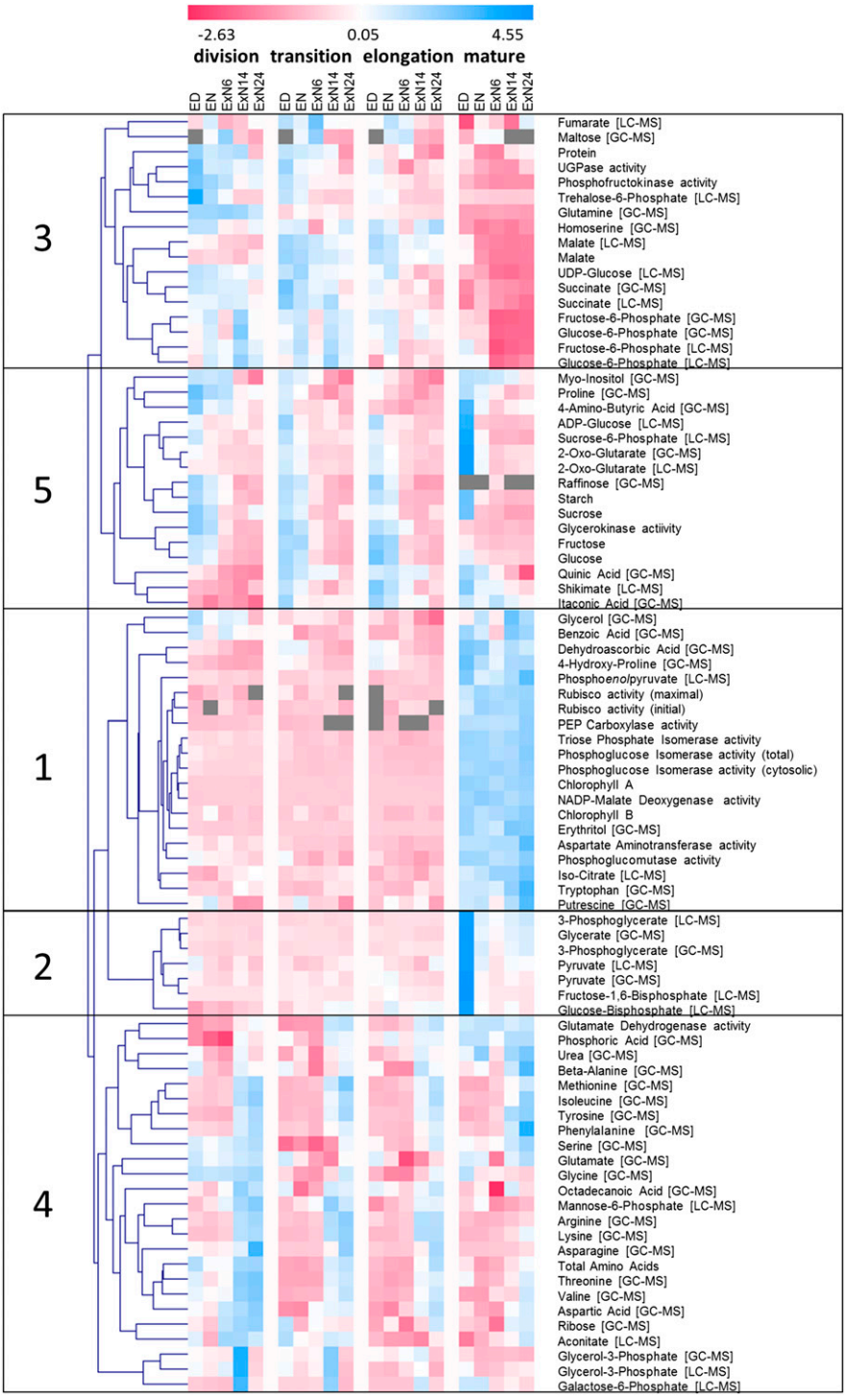

Figure 2. Hierarchical clustering of metabolic traits over the carbon starvation time course. Sixty-four different metabolites and in the in vitro maximum activity of 11 different central metabolic enzymes over the C starvation time were determined in the four leaf zones indicated in Figure 1A. Measurement values for each trait were z-score transformed (see "Materials and Methods") to make the range of values comparable between individual traits. The normalized metabolic traits were then hierarchically clustered to identify traits with similar trajectories of change over the time course and/or between the studied leaf regions. Clustering was performed with TMEV version 4 (Saeed et al., 2003) using Euclidean distance as similarity measure. Traits were determined by different measurement platforms indicated in cornered brackets (for more details, see "Materials and Methods"). In some cases, different properties of an enzyme were measured. This is indicated by round brackets. Details can be found in the "Materials and Methods" section. Gray fields, missing data points. Trait values can be found in Supplemental Datafile S1. Individual plot of all traits can be found in Supplemental Datafile S2.

our quantitative measurements (Fig. 3B), in the mature leaf, starch accumulated during the day and was almost completely degraded during the night. In contrast, starch reserves in the growth zones at the leaf base did not show any visual differences in iodine staining intensity between ED and EN, remained high at 6hExN, and then decreased. The middle of the leaf was essentially starch-free at all times.

In summary, the temporal dynamics of metabolites during the C-depletion time course vary between leaf zones, in particular (1) C depletion occurs more rapidly in mature than in growth zones, (2) there is a partial recovery of Suc toward the end of our extended night time course level in the growth zones but not in mature tissue, and (3) protein decreases in growth zones during the last part of the extended night.

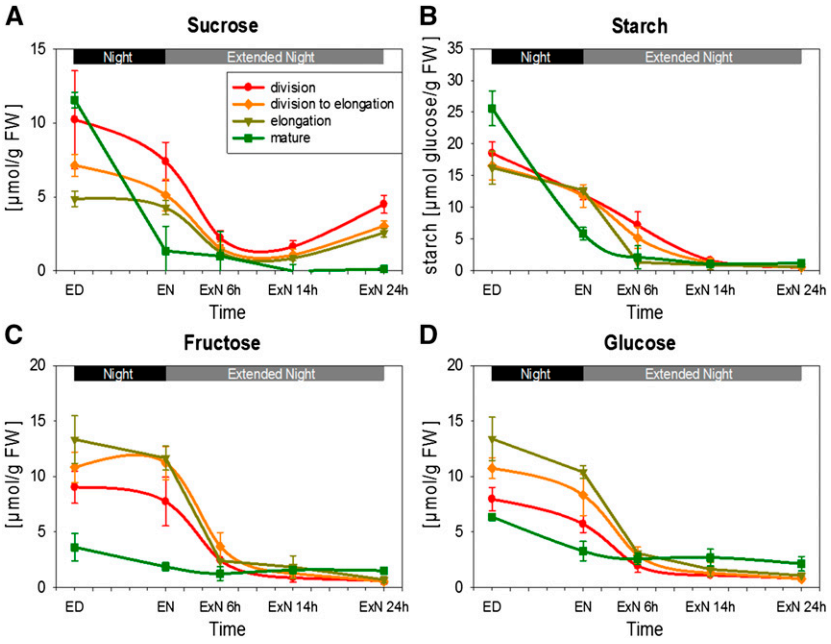

Figure 3. Changes in major carbohydrates over the carbon starvation time course. Carbohydrate levels in the four leaf zones indicated in Figure 1A sampled over the carbon starvation time course were determined by photometric assays (see "Materials and Methods"). Starch values are given as µmol Glc units/g fresh weight. Each data point represents the mean of three biological replicates. Error bars: SD. A, Suc; B, Starch; C, Fru; D, Glc. *Indicates that the rise in Suc between 14hExN and 24hExN is statistically significant in all three growth zones (P value < 0.05). ED, End of day; EN, end of night; ExN 6h/14h/24h, extension of the night by 6 h/14 h/24 h. x axis ticks indicate 2 h intervals.

Expression Profiling in the Leaf Zones during the C Depletion Time Course

We conducted transcript profiling to gain further insights into the response to C depletion in the division, elongation, and mature zones (R1, R3, and R4, respectively). For these studies, we used the maize Affymetrix array. This array was designed before the release of the full maize genomic sequence (Schnable et al., 2009). Comparison of the probesets with maize genome release B73 RefGen v.2 5b (ftp://ftp.gramene.org/pub/gramene/maizesequence.org/release-5b/) revealed that many probe sets significantly match more than one maize gene model, and some do not match any gene model. We filtered the array dataset to retain only those probesets that match significantly to a single maize gene model and to retain only one probeset per gene model. Of 17,734 probesets, only 3583 passed this filter. For these 3583 genes, an updated Mapman mapping was assembled. The complete filtered and RMA normalized gene expression dataset with annotation is provided in Supplemental Datafile S4.

The expression dataset was analyzed using analogous approaches to those used for the metabolic dataset. PCA (Fig. 1D) gives a picture initially reminiscent to that for metabolic profiles. PC1 captured ~70% of the variation and grouped samples according to the developmental gradient; samples from the mature tissue were set strongly apart from the elongation and division zones. PC2 captures ~10% of the variation and separates the samples along the C depletion time course, with separation being largest in the mature zone and smaller in the growth zones. Whereas the ED and EN samples are clearly separated in the mature tissue, the ED and EN samples from the growth zones are superimposed, indicating that the change in global gene expression during the night is much smaller in the growth zones. Interestingly, in the growth zones, the order of the 14hExN and 24hExN samples along PC2 is reversed, showing that between 14 and 24 h into the extended night, global gene expression in the growth zones reverts to a state that is more similar to that at an earlier stage of the C depletion time course. This resembles the pattern seen for Suc (Fig. 3A). A similar picture emerges using two other visualizations of the global expression pattern.

A similar picture emerges using two other visualizations of the global expression pattern. First, for each leaf region, we correlated the expression profile at ED with the expression profile at each subsequent time point (Fig. 1E). We term this the "expression profile change." This visualization illustrates that the global changes in expression are less pronounced and occur more slowly in growth zones than in mature tissue, as already seen for metabolites. It also reveals a partial, but significant (P values $<$ 1E-4) reversal in the cell division and elongation zones between 14hExN and 24hExN time point, as seen in PC2 (Fig. 1D). In the second approach, we calculated, analogous to the "mean metabolic change relative to ED," "mean expression change relative to ED" (Supplemental Fig. S4), i.e. we calculated for each leaf region, the differences in expression for each probeset between ED and the other time points. The differences were then averaged across all probesets for a given time point and leaf region, after converting negative to positive values. This gives a very similar picture to the "expression profile change" obtained by correlating the expression profiles. An ANOVA showed that most of the studied genes show significant expression changes between the leaf regions (3441 of 3583 genes) and/or over the C-depletion time course (2771 genes), and that a large proportion of the profiled genes show a significant interaction between the leaf

region and C-depletion time course effects (2381 genes; Supplemental Fig. S5).

Differences in Transcript Abundance between the Studied Leaf Zones Are in Accordance with the Leaf Zone Identities and Largely Persist upon C Starvation

We next compared expression between leaf zones. We first asked which functional classes of transcripts are up- or down-regulated in a coordinated way in a given leaf zone compared to average transcript abundance over all zones (Fig. 4A). To this purpose, we normalized the abundance of each probeset at ED to its average abundance over the three leaf regions at ED. Then we used the software Pageman (Usadel et al., 2006) to test by Wilcoxon test which functional classes are significantly up- or down-regulated in each leaf region. *P* values were corrected for multiple testing by the Benjamini-Hochberg algorithm (Benjamini and Hochberg, 1995). The results of this analysis are in accordance with the presumed identities of the sampled leaf regions. The developmental gradients at ED resemble those in previous studies of material harvested in the light (Pick et al., 2011; Wang et al., 2014). Transcripts related to photosynthesis and isoprenoid biosynthesis, and chloroplast ribosomal proteins were low in the division and expansion zones and highest in mature tissue. Transcripts for DNA synthesis, chromatin structure, cell organization, RNA processing, and regulation of transcription were highest in the division zone and lowest in mature tissue. Transcripts for cytosolic ribosomal protein encoding genes were higher in the growth zones than mature tissue. Transcripts for cell wall precursor synthesis were highest in the elongation zone, where there will be a high demand for cell wall synthesis. Transcripts for the proteasome, protein glycosylation, and protein folding were also highest in the elongation zone. These developmental expression gradients were also seen at EN and even during ExN, although some of differences become less marked—for example, for genes related to isoprenoid metabolism, RNA processing and regulation of transcription—and the gradients for chloroplast ribosomal proteins were abolished (Supplemental Fig. S6). Thus, developmental expression gradients are conserved during the diurnal cycle and largely persist under C starvation.

Differential Response of Transcript Abundance in the Leaf Zones to C Depletion

We next asked which functional classes of transcripts increase or decrease in a coordinated way during the C-depletion time course. We calculated, for each probeset and leaf region, the change in transcript abundance between ED and each subsequent time point, and used Pageman's Wilcoxon test (with correction for multiple testing by the Benjamini-Hochberg algorithm) to identify functional classes that are significantly up- or down-regulated at a given time compared to ED (Fig. 4B).

This analysis gave several insights: First, transcripts for functional classes related to anabolic processes and growth, such as photosynthesis, DNA-synthesis, cell organization, amino acid synthesis, and protein synthesis decreased during the C depletion time course. Second, there were marked differences between the leaf regions. Transcripts related to photosynthesis and isoprenoid metabolism—chloroplast ribosomal proteins were down-regulated only in mature tissue. Downregulation of amino acid synthesis and cytosolic ribosomal proteins was also strongest and occurred earlier in mature than growing tissue. Indeed, there was no significant down-regulation of genes assigned to cytosolic ribosomes in the division zone, even though expression was much higher than in mature tissue (Fig. 4A). On the other hand, the decrease of genes for DNA synthesis was limited to the growth zones. Third, transcripts for catabolic pathways (lipid degradation, amino acid degradation, protein degradation by the ubiquitin pathway, including E3 ligases and especially the RING class) increase during the C depletion time course. However, whereas transcripts for the ubiquitin pathway showed a sustained increase in mature tissue, they peaked at 14ExN and then partly reversed in the elongation zone and almost completely reversed in the division zone.

Integration of Transcriptional Responses with Metabolite Levels and Enzyme Activities

The increase of transcripts for amino acid degradation is consistent with increased protein and amino acid catabolism during ExN, which was already proposed based on the observed rise in amino acid levels. A strong induction of the Glu-DH-encoding transcript *ZmGDH1/3* (gene codes, orthology, and naming information: see Supplemental Datafile S5) in the growth zones in ExN preceded the increase in Glu-DH activity (Supplemental Fig. S7, A and B). The steady increase of *GDH1/3* transcript up to 14hExN in the growth zones is reversed at 24hExN, showing the pattern of partial reversal of expression change in the growth zones at 24hExN that was seen in global visualizations (Fig. 2E). Arabidopsis orthologs (*AtGDH1*, *AtMIOX2*, *AtMIOX4*) are also induced upon C starvation (Melo-Oliveira et al., 1996; Gibon et al., 2006; Kim and von Arnim, 2006; Osuna et al., 2007; Usadel et al., 2008; Alford et al., 2012) and are required in the starvation response in Arabidopsis (Miyashita and Good, 2008; Alford et al., 2012).

The decrease in myoinositol in the C-depletion time course (Supplemental Fig. S7D) is accompanied by very strong induction of *ZmMIOX* in all leaf zones, especially the division zone (Supplemental Fig. S7C). *ZmMIOX* is the only identified maize gene encoding the myoinositol catabolizing enzyme myoinositol oxygenase. *ZmMIOX* was induced during the night in all analyzed leaf regions and further induced in the mature tissue up to 6hExN and in the growth zones up to 14hExN, before declining slightly. The up-regulation of *ZmMIOX* in the cell division zone (>100-fold) was the strongest observed change in transcript abundance in our experiment. There was also a stronger decrease in

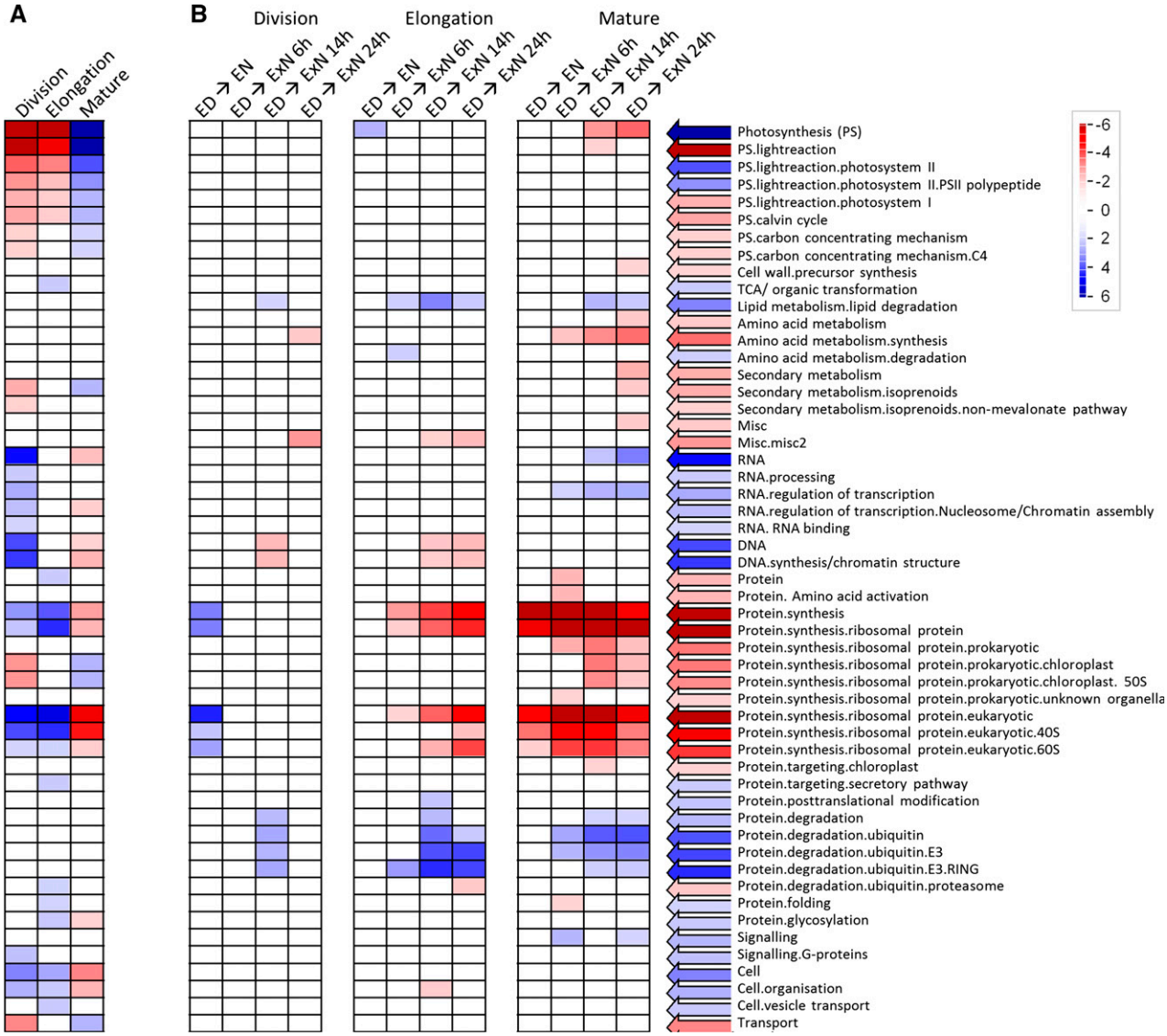

Figure 4. Changes in transcript abundance for functional classes of transcripts. A, Over the leaf gradient; B, over the C starvation time course. A, Comparison of gene expression between the leaf zones at ED. For each probeset, the expression values over the three leaf zones were normalized to their mean. Pageman (Usadel et al., 2006) with Wilcoxon test statistics and Benjamini-Hochberg multiple testing correction (Benjamini and Hochberg, 1995) was used to identify functional classes (Mapman bins) that are significantly up- or down-regulated compared to mean expression in a given leaf region. B, In each leaf region, gene expression at each time point was compared to expression at ED. Wilcoxon test with Benjamini-Hochberg multiple testing correction was used to identify functional classes of transcript that are significantly up- or down-regulated in this comparison. ED, End of day; EN, end of night; ExN 6h/14h/24h, extension of the night by 6 h/14 h/24 h; blue, up-regulation; red, down-regulation.

myoinositol during C starvation in the growth zones than mature tissue. However, the strong decrease in the cell division zone did not start until after 6hExN, which matches the delay in induction of *ZmMIOX* in this zone.

Another very well described C starvation marker in Arabidopsis is *Asn synthetase1* (*AtAsn1*, *AT3G47340*; Lam et al., 1994, 1998; Fujiki et al., 2001; Osuna et al., 2007; Hanson et al., 2008). *GRMZM2G093175* (identified as the maize ortholog of *AtAsn1* with 74% ID by OrthoMCL; Li et al., 2003) did not show a significant expression change in the C-depletion time course (Supplemental Fig. S8A). Other maize genes with high orthology to *AtAsn1* (*GRMZM2G074589*, *GRMZM2G053669*, *GRMZM2G078472*) that are not covered in our dataset might explain the accumulation of Asn.

Response of Transcripts Encoding Potential C-Signaling Components

We inspected the abundance of transcripts that encode putative maize orthologs of C-signaling components. Our dataset included two hexokinase

transcripts, *ZmHXK1/GRMZM2G104081* and *ZmHXK5/GRMZM2G051806*, according to Zhou et al. (2013). In mature tissue, *ZmHXK1* and *ZmHXK5* expression rose during ExN up to the last time point, while in the growth zones, expression rose until 14hExN and declined at 24hExN (Supplemental Fig. S8, B and C). This pattern resembles the patterns observed for *GDH1/3* and global gene expression. A similar pattern was observed for *GRMZM2G107867*, one of three maize genes encoding proteins highly orthologous to the Arabidopsis KIN10 and KIN11 catalytic subunits of SnRK1 (Supplemental Fig. S8D). A putative maize homolog (*GRMZM2G025459*) to the regulatory beta-1 subunit of SnRK1 also showed a marked response; in mature tissue, the transcript rose significantly between ED and EN, rose further at 6hExN and then plateaued, while in growth zones the rise was delayed, starting after EN in the elongation zone and after 6hExN in the division zone (Supplemental Fig. S8E).

Response of Whole-Leaf Elongation Rate during the C-Depletion Time Course

To monitor growth, we measured the elongation rate of leaf 9 and (next section) analyzed polysome loading as a proxy for protein synthesis. Leaf elongation was determined using a rotary resistor- (RRT) based apparatus (Ben-Haj-Salah and Tardieu, 1995; Wiese et al., 2007; Poiré et al., 2010; Supplemental Fig. S9A). We monitored elongation rate in 10 randomly chosen plants from the experiment in which samples were taken for metabolite and transcript analyses (Fig. 5A). Elongation growth was measured for a complete night and light period before the first sampling time point at ED, and then during the night and ExN. Coinciding with the switches from dark to light and light to dark are sharp depressions and peaks, respectively, in the extension rate. The growth chamber used for our experiments requires a short light dimming period before the switch from light to darkness; thus, the narrow peaks occurred shortly before onset of total darkness. Similar peaks have been observed for mature maize leaves (Tang and Boyer, 2008) and Arabidopsis rosettes (Apelt et al., 2015) and are presumably due to rapid turgor responses to the sudden changes in light intensity, temperature, and air humidity. We ignore them in the following account of the growth pattern.

In the light period, elongation rates rose to a maximum 5 to 6 h after dawn, decreased later in the light period, and continued at a constant but still high rate during the night (Fig. 5A). This resembles earlier studies (Tang and Boyer, 2008). After onset of the extended night, elongation continued for about 6 h at approximately the same rate as during the night, and then gradually decreased to a lower rate that was approximately one-third of that in the night. From 18 to 20 h onwards, the elongation rate showed a slight recovery, weaker but reminiscent of the recovery seen for Suc and global gene expression.

A second independent experiment showed a very similar response pattern in leaf 8 (Supplemental Fig. S9B). In this experiment, elongation was also tracked after returning plants to a light-dark cycle. Growth increased gradually over about 6 h to reach a maximum that was slightly lower than in a regular light-dark cycle and remained approximately constant until the end of the light period, rather than declining. Variation between plants was higher in the first light period after the ExN treatment. The following dark period and the first hours of the second light period after the ExN resemble the pattern before the ExN.

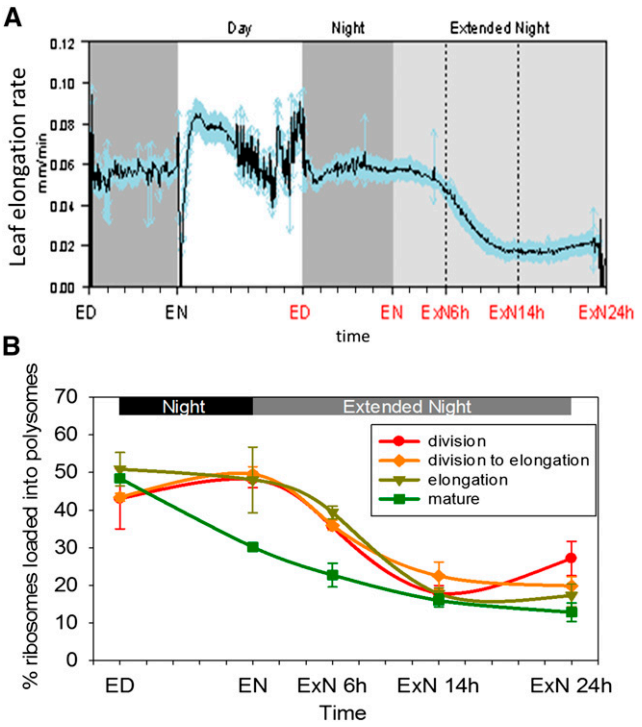

Figure 5. Response of leaf elongation rate and polysome loading in four zones of the growing maize leaf blade to a C starvation time course. A, Leaf elongation rate of leaf 9 was measured for 10 plants with an RRT-based device (Supplemental Fig. S9A) during the same experiment when samples for metabolic and transcriptional measurements were taken. Resolution of 5 min. Mean of the 10 measured plants (black line) and SD for each time point (blue arrows) are depicted. B, Suc density gradient fractionation was used to determine in each sampled leaf zone (see Fig. 1A) the proportion of ribosomes loaded into polysomes as a proxy for protein synthesis rate. Each data point represents the mean of two or three biological replicates. Error bars: SD. ED, End of day; EN, end of night; ExN 6h/14h/24h, extension of the night by 6 h/14 h/24 h. *x* axis ticks indicate 2 h intervals.

Leaf-Zone-Resolved Changes in Polysome Loading during the C Depletion Time Course

Protein synthesis is a major component of cellular growth (Warner, 1999; Rudra and Warner, 2004). Qualitative information about the rate of protein synthesis can be obtained by using Suc density gradient centrifugation to analyze polysome loading (Kawaguchi et al., 2003; Piques et al., 2009; Pal et al., 2013). In Arabidopsis rosettes, which consist of a large proportion of mature

leaf tissue, polysome loading is high at the end of the day, considerably lower at the end of the night, and decreases further during an extension of the night (Piques et al., 2009; Pal et al., 2013).

We investigated polysome loading in each maize leaf zone during the C-depletion time course. In mature tissue, polysome loading decreased between ED and EN and decreased further at 6hExN and 14hExN (Fig. 5B), resembling the response in Arabidopsis. In contrast, in growth zones, polysome loading remained high (elongation zone) or even increased slightly (transition zone, division zone) at EN compared to ED and was only slightly decreased at 6hExN. At 14hExN, polysome loading in the growth zones fell to values similar to or only marginally higher than in the mature zone. In the division zone, polysome loading increased again at 24hExN, resembling the pattern seen for Suc, global gene expression, and elongation growth.

Protein synthesis depends not only on the proportion of ribosomes loaded into polysomes, but also on total ribosome abundance. We compared total absorption at A_{254} between samples, summing the areas of free ribosome and polysome peaks in the fractionation profile (see "Materials and Methods"). This indicated that ribosome abundance was up to 2-fold higher in growth zones than mature tissue. However, there were no major changes in ribosome abundance in any of the leaf regions during the C-depletion time course (Supplemental Fig. S9C).

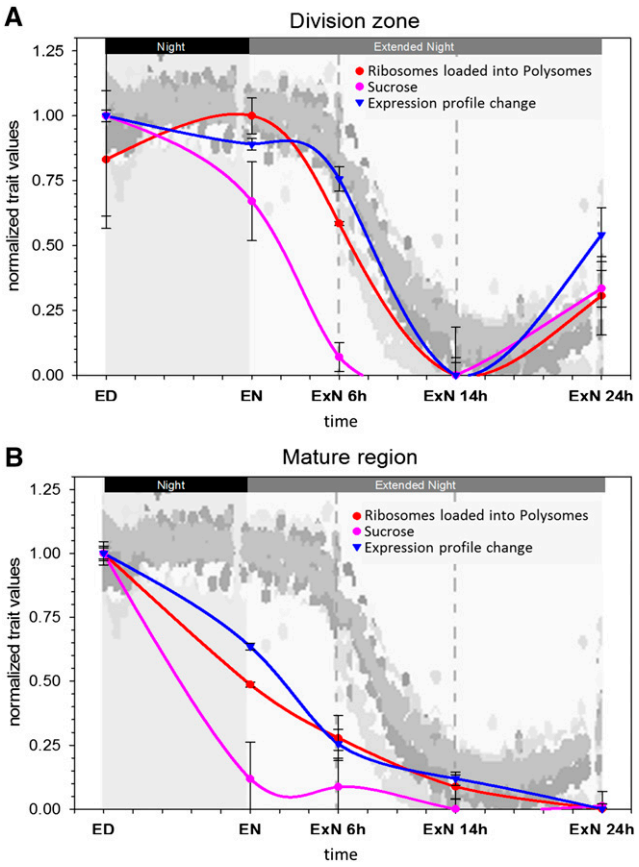

Figure 6. Overlay of the responses of different traits to a C starvation time course in two zones the growing maize leaf blade. The responses of polysome loading (Fig. 5B), Suc concentration (Fig. 3A), and expression profile change compared to ED (Fig. 1E) in (A) the cell division zone and (B) the mature tissue were each normalized to a distribution between 0 (lowest value) and 1 (highest value). These graphs were superimposed onto the plot of whole-leaf elongation rate over the same time course (Fig. 5A), allowing a comparison of the patterns. Whole-leaf elongation patterns for 10 individual replicate leaves measured in parallel are indicated by different tones of gray. Error bars, SD. Time points: ED, end of day; EN, end of night; ExN 6h/14h/24h, extension of the night by 6 h/14 h/24 h. *x* axis ticks indicate 2 h intervals.

Growth Is Coordinated with C Resources in the Growth Zones

Figure 6, A and B, compare, for the cell division zone and mature leaf zone, the temporal changes in Suc content, polysome loading, the "gene expression profile change" over the time course obtained by correlating expression profiles at each time point against ED (see Fig. 1E and explanation in legend), and the rate of whole leaf extension. In each leaf region, the temporal patterns of polysome loading and global gene expression were quite similar to each other and follow, after a short delay, the change of Suc content. All three parameters change earlier and more dramatically in mature tissue than the cell division zone. Further, all three traits show a partial recovery at 24hExN in the cell division zone. A similar picture is seen for these processes in the elongation zone, except that the Suc recovery is not mirrored by a recovery of polysome loading (Supplemental Fig. S10).

The responses of the whole leaf elongation rate match the response of polysome loading and gene expression in the cell division zone and follow, after a short delay, the change of Suc in the growth zones. There is little relation between the change of Suc in the mature tissue and the responses of polysome loading and gene expression in the growth zones, or the rate of whole leaf elongation. In the mature leaf zone, Suc content decreases rapidly during the night, while whole leaf elongation rates remain high and polysome loading in the division zone even rises between ED and EN. Between 14hExN and 24hExN, Suc remains low in the mature leaf zone and polysome loading in the division zone and whole leaf elongation partially recover. Summarizing, processes required for growth, such as leaf elongation and growth zone protein synthesis, are linked to C availability in the growth zones rather than the mature tissue.

Other major C resources, such as the monosaccharides Glc and Fru, did not recover at 24hExN (Fig. 3). A small number of other metabolites displayed a partial recovery (shikimate, Suc-6-phosphate), but not as pronounced as Suc (Fig. 2; Supplemental Datafile S2). This indicates that growth may be driven by the local Suc level. The Suc signaling metabolite T6P did not show significant recovery at 24hExN (Fig. 2; Supplemental Datafile S2, see also discussion of T6P later on).

Estimation of Starch Dilution by Growth in the Night and Extended Night

In a growing tissue, the starch content depends not only on the rates of starch synthesis and degradation, but also on the rate of dilution by tissue growth. Using the recorded leaf elongation data, we estimated how starch would be diluted by growth between successive time points.

This was estimated for the summed starch content in the transition and the elongation zones (R2 and R3, i.e. 1.5 cm–4.5 cm above the ligule), since elongation in R1 is presumably lower and inhomogeneous, while elongation in R2 and R3 is can be assumed to be roughly linear (see Meiri et al., 1992). Elongation in zone R3, where cells are only elongating, but not dividing, can be estimated from the cell length profile (Supplemental Fig. S1B) and comprises approximately 25% of total cell elongation. Under the assumption that elongation rate is R2 is similar to R3, we estimate that approximately 50% of whole leaf elongation occurs within the region covered by R2 and R3. Based on this estimated elongation rate, we estimated for each 5 min interval a notional rate of dilution of starch by growth, assuming that there was no starch synthesis or degradation, and compared these notional trajectories with the measured starch content at the beginning and end of each time interval (Supplemental Fig. S11). Between ED and EN, the estimated dilution by growth was almost 3-fold higher than the actually decrease in starch content per unit fresh weight. Even if R2 and R3 represent less than 50% of the total leaf elongation or the elongation rate between R2 and R3 is not quite homogenous, results change only marginally. For example, if we assume that R2 + R3 covers only 40% of overall leaf elongation, the estimated starch decrease by dilution is still more than twice of the observed starch decrease. Thus, these calculations indicate that there was no net starch degradation during the night in zones R2 and R3; on the contrary, C import and starch synthesis may be required to maintain starch at the level measured at the end of the night. During the extended night, starch levels in these zones decreased faster than expected through dilution by growth, indicating that the starch was being degraded. In line with this, there was a transient rise in the level of the starch degradation intermediate maltose in the growth zones at 6hExN (Supplemental Fig. S12).

Modeling of the Relation between C Resources in the Leaf and C Required for Leaf Growth

We used a C balance model to ask if the local C reserves in the growth zones and/or the C reserves in the mature leaf part are large enough to support the observed growth during night and ExN. To do this, we compared, for each time interval, the amount of C that becomes available from remobilization of C reserves in the mature leaf and in the sampled growth zones with the amount of C that is required to fuel the observed rate of leaf growth (Fig. 7; Supplemental Datafile S3 for more details).

The net C reserves used during each time interval were calculated from the difference in sugars (Glc, Fru, Suc) and starch content between the start and end of the time interval. For simplicity, resources in the three growth zones were summed. However, only a small section of the mature leaf part was sampled. We therefore used the area containing transitory starch at the ED, as determined by iodine staining, to interpolate the total C in the mature part of the leaf. For the mature tissue, we also included on the credit side C that becomes available through the decrease in amino acids, malate and fumarate over the time course (labeled "other C sources mature" in Fig. 7); the contribution of these sources in the growth zones is very small and was therefore ignored.

The C required for leaf growth was estimated in the following way: We used the elongation increment per time interval (cm) to calculate how much leaf dry weight has to be synthesized during each interval. As a basis, we used experimentally determined dry weight/cm data for EN, adjusted for each time point by the cumulative change in metabolite and protein content compared to that at EN (Supplemental Datafile S3). We used a value of 1.055 g Suc required as C source per g dry weight (Penning De Vries, 1975) to estimate how much C is required for the calculated increment in dry weight. The observed rise in amino acid levels at the 14hExN and 24hExN time point and partial recovery of Suc in the growth zones at the 24hExN time point were entered as additional C requirements (Fig. 7: "C for AA rise and sucrose recovery"). Measurements of the respiration rate in the mature leaf area during the night and extended night was used to account for respiratory C loss in the mature tissue (Supplemental Datafile S3; Fig. 7: "respiration (mature)"). Respiration in the growth zones required to provide energy for biosynthetic processes is already accounted for in the C-budget for dry weight synthesis. We also estimated, based on the rate of photosynthesis in the light, the net C gain in the light period preceding the night and ExN. This value was compared to the amount of C required for the accumulation of the C reserves and the growth observed during the day (Fig. 7).

Our C balance model leads to several conclusions: First, in the light leaf 9 assimilates slightly more C than is required for growth and accumulation of C reserves. This small discrepancy may be due to assumptions involved in our calculations, or a small amount of C might be exported from the leaf during the day. Second, during the night, most of the C mobilized within leaf 9 derives from the mature part of the leaf and virtually none from the sampled growth zones, while during the first phase of ExN (EN-6hExN) 3-fold more C is remobilized from the sampled growth zones than the mature tissue (Fig. 7; Supplemental Datafile S3). Third, it seems likely that leaf 9 is not self-sufficient during the night or ExN. The C remobilized from the profiled reserves in leaf 9 accounts for only 20% of the

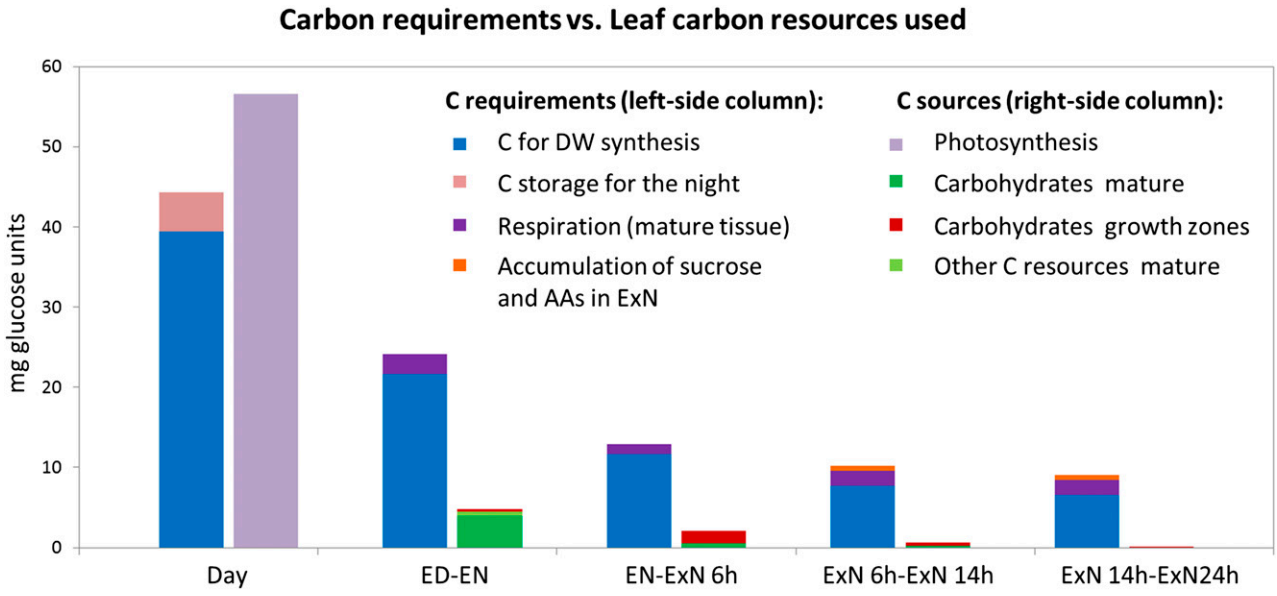

Figure 7. Comparison of C requirements for leaf growth and maintenance in the sampled leaf zones with C provided through depletion of profiled C reserves. This figure compares, for each leaf interval, the amount of C needed to support the measured leaf growth and respiration in the mature leaf area to the amount of C provided from C reserves in the growth zones and the mature leaf tissue and, during the day, photosynthesis. C provided from reserves was estimated by calculating the difference in these resources at the beginning and end of each time interval. Values were summarized for the three growth zones and interpolated for the total mature area of the leaf based on iodine staining for starch. The middle part of the leaf is not accounted for. "Carbohydrates" refers to starch, Suc, Glc, and Fru; "other C resources" accounts for malate, fumarate, and amino acids. "Accumulation of sucrose and AAs in ExN" refers to the increase in the levels of amino acids (AAs) and Suc in the growth zones toward the end of the extended night time course, which will represent an additional C requirement at this time. Photosynthesis and respiration of the mature leaf tissue was determined by gas exchange measurement (Supplemental Fig. S13). For details of the calculations, please refer to the main text and Supplemental Datafile S3. Time points: ED, end of day; EN, end of night; ExN 6h/14h/24h, extension of the night by 6 h/14 h/24 h.

estimated requirement for C for growth during the night, about 18% in the interval between EN and 6hExN, 8% in the interval between 6hExN and 14hExN, and 2% in the interval between 14hExN and 24hExN. This last conclusion is tentative because we did not measure carbohydrate reserves in all of the elongation and maturation zone; however, iodine staining (Fig. S3) indicated at least for starch that the content is low and unlikely to explain this very large deficit of C for growth.

Starch Reserves Are Successively Depleted during Night and an Extended Night

These calculations indicated that much of the C for growth of leaf 9 during the night and ExN derives from outside leaf 9. We therefore investigated C reserves at a whole-plant level. To do this, we performed iodine staining in all leaves and in vertical stem sections at several time points during the C-depletion time course (Fig. 8). At ED, there were considerable amounts of starch at the bases of growing leaves, in the mature zones of all leaves, and in the stem. At the EN, there was much less starch in the mature leaf areas, especially those of older leaves, but starch staining was comparable to ED at the base of young growing leaves and in the stem in the leaf nodes. During the extended night, starch was successively depleted in the leaf nodes, first in the oldest and last in the youngest. Even 24 h after start of the extended night, there were still traces of starch left in the youngest leaf nodes. These results highlight differences in the temporal pattern of starch depletion during the night and ExN between different tissue and organs in the maize shoot and indicate that starch in older leaves and the stem provides a source of C for younger leaves during the night and ExN.

Relation between Suc and T6P in Growing and Mature Leaf Zones

We next investigated the response of T6P in the different leaf zones (Fig. 9). T6P has been described as a signal of Suc status that links C availability with growth and development (Lunn et al., 2006, 2014; Yadav et al., 2014). In whole Arabidopsis seedlings and rosettes, T6P and Suc vary in parallel, with a ratio of about 0.1 to 0.3 nmol T6/μmol Suc (Lunn et al., 2014; Yadav et al., 2014). A similar ratio has been reported in maize seedling leaf tissue (0.1 nmol T6P/μmol Suc; Horst et al., 2010).

At ED, T6P levels in the cell division, transition, and elongation zone were almost 20-, 10-, and 5-fold higher than in mature zone (Fig. 9A). As already mentioned, the Suc level at ED in the cell division zone was marginally lower and that in the transition and elongation zones was about 40% and 60% lower, respectively, than in mature

tissue (Fig. 3A). The T6P:Suc ratio at ED was about 0.04×10^{-3} (unitless) in the mature zone and rising to 0.4, 0.5, and 0.9×10^{-3} in the elongation, transition and cell division zones, respectively (Fig. 9B). During the night and the ExN, T6P decreased strongly in all leaf zones. However, in the growth zones the decrease in T6P was much larger than the decrease in Suc. This resulted in a decline in the T6P:Suc ratio in the growth zones during the ExN, so that by 14hExN the ratios in all growth zones resembled those in mature tissue at ED and EN. The T6P:Suc ratios in the mature tissue at time points during ExN could not be determined, due to the very low Suc levels and proportionally large measurement error at these time points. There was only a small nonsignificant increase of T6P at 24hExN, when Suc rose in the growth zones (Fig. 9A, inset).

Identification of Transcripts with Characteristic Temporal Response Patterns

Transcripts with similar temporal responses to Suc content, polysome loading, or leaf elongation could be involved in signaling or mediating downstream responses to C availability. We used two strategies to search for such transcripts.

Strategy 1 employed stepwise filtering (see "Materials and Methods") to identify transcripts with a qualitatively similar recovery response to that of Suc and the growth traits (i.e. unidirectional change until 14hExN and partial recovery at 24hExN; see Fig. 6A). We identified transcripts with this pattern in each leaf zone (Fig. 10A; see Supplemental Datafile S4: "patterns" for lists of probesets). However, many more transcripts show this "recovery pattern" in growth zones than mature tissue (Fig. 10A). There is a highly significant overlap between transcripts showing the recovery pattern in the division and elongation zones (Fisher's exact test; P value $< 10^{-16}$) but no significant overlap between these sets and transcripts showing the recovery pattern in mature tissue. For example, *ZmHXK1*, *ZmHXK5*, *ZmGDH1/3*, and Zm*KIN10/11* transcripts (see above) were identified as showing the recovery pattern in the growth zones but not in mature tissue.

Strategy 2 employed correlation analysis. We first identified all probe sets that changed significantly over the time course (ANOVA, Benjamini-Hochberg corrected

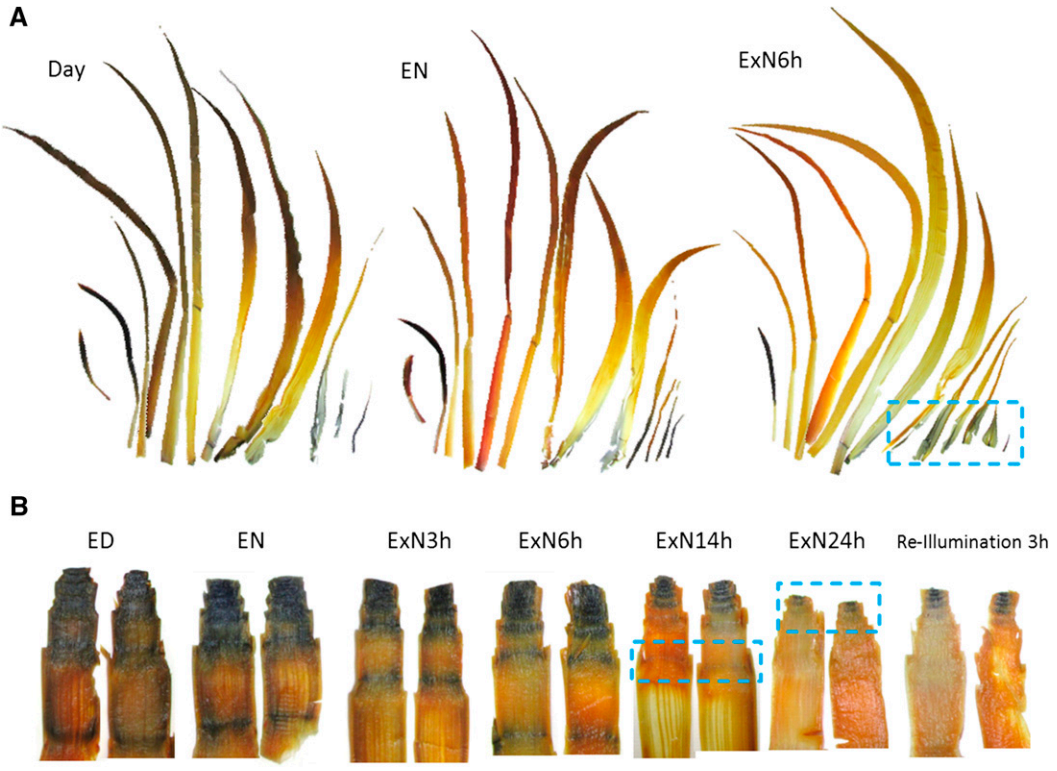

Figure 8. Shoot-wide localization of starch reserves in maize plants sampled over the C starvation time course. A, Starch staining of all leaves of a 3.5-week-old plant (from left: oldest, to right: youngest) sampled at different time points over a C starvation time course. B, Starch staining of vertical stem sections from plants sampled at different time points over a C starvation time course. Stained sections from two different plants are shown at each time point. Blue boxes indicate starch retained into the extended night at the bases of young leaves (A) and the successive depletion of starch in the leaf nodes from bottom (nodes of oldest leaves) to top (youngest) during the extended night (B). Time points: Day, 4 h before the end of the day; ED, end of day; EN, end of night; ExN 3h/6h/14h/24h, extension of the night by 3 h/6 h/14 h/24 h; Reillumination 3 h, after 24 h of extended night, the plants were reilluminated and samples taken 3 h into the day.

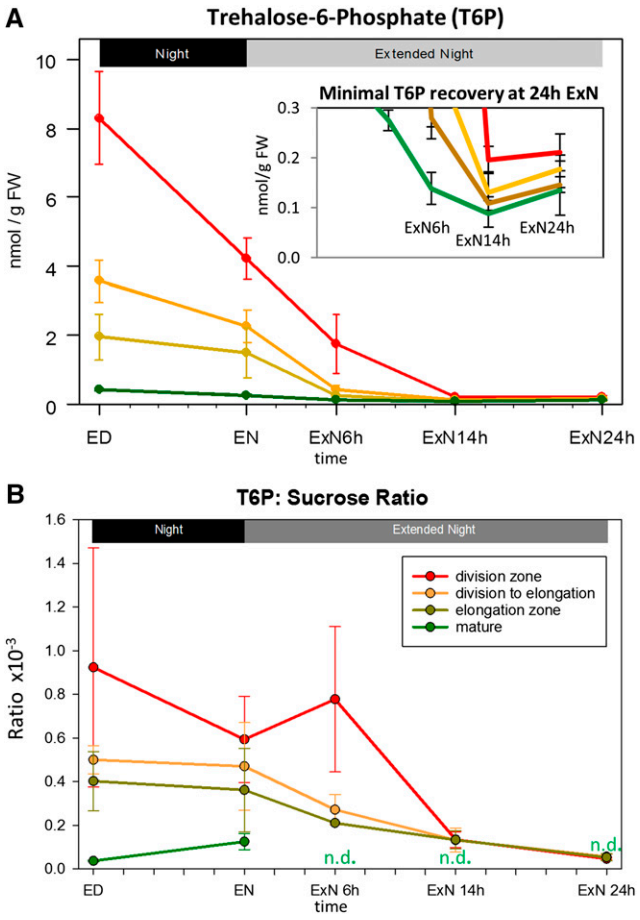

Figure 9. The response of T6P levels and T6P:Suc ratio in four zones of the growing maize leaf to a C starvation time course A, T6P was determined in the leaf zones indicated in Figure 1A by liquid chromatography-mass spectrometry triple quad analysis (Lunn et al., 2006). Values are averages of three biological replicates; error bars: SD. Inset: Different *y* axis scale is used, so that small changes over the last three time points are visible. B, The ratio of T6P to Suc (Suc: Fig. 3A) was calculated for the biological replicates for each leaf region and time point (typically 3) individually. Mean and SD of these values are shown. ED, End of day; EN, end of night; ExN 6h/14h/24h, extension of the night by 6 h/14 h/24 h. *x* axis ticks indicate 2 h intervals. N.d., Ratio not determinable due to very low input values and high error.

P value < 0.001) and then calculated the Spearman rank correlation between each transcript and Suc content, polysome loading, or the rate of leaf elongation. Spearman correlation was used because it is suited to detect nonlinear relationships. This approach was not well suited to test relationships for each leaf zone individually, due to limitations of statistical power of the Spearman method with only five data points. For this reason, analyses were performed over (1) all three leaf zones and (2) the two growth zones. Correlations were calculated using raw measured values for all traits or after z-score normalizing values for each leaf zone individually and combining them to aid identification of transcript pairs that correlate in each of the tested leaf zones but whose ratio differs between zones. We assembled, for each target trait, a merged list of transcripts that correlated to the trait significantly at $R > 0.9$ or < -0.9 in one or more of the correlation approaches. The results are summarized in Figure 10B, and the probesets are listed in Supplemental Datafile S4. This approach distinguished between transcripts that correlate more strongly with Suc and whose change precedes the change in growth and transcripts that change in parallel with growth. Transcripts that correlate with Suc may represent early regulatory responses that link the C status to later responses of growth and metabolism.

In line with the visualization in Figure 6, more transcripts correlate with elongation rate and polysome loading (417 and 568 transcripts, respectively) than Suc content (128 transcripts). There was strong overlap between the transcripts that correlated to elongation rate and to polysome loading (Fisher test, *P* value $< 10^{-16}$) and extremely small overlap of these two sets with the transcripts that correlated to Suc (*P* values $< = 8.4*10^{-3}$ for underrepresentation; Fig. 10B). *ZmHXK5*, *GDH1/3*, and *MIOX1* are in the set that are negatively correlated to Suc, while *ZmHXK1* is negatively correlated to polysome loading.

We next tested for over-/underrepresentation of functional classes (Mapman bins) in the gene sets identified by both strategies (Fig. 10C), doing this separately for transcripts that changed in the same ("positive," light green in Fig. 10A) or opposite ("negative," dark green in Fig. 10A) direction the target traits. The analysis was performed with Pageman (Usadel et al., 2006), using Fisher statistics and multiple testing corrections by the Benjamini-Hochberg algorithm (Benjamini and Hochberg, 1995). Different functional categories were overrepresented in different leaf zones (Fig. 10C). Functional classes related to DNA synthesis and chromatin structure were overrepresented among transcripts showing a positive recovery pattern in the division zone, classes related to lipid metabolism and amino acid degradation were overrepresented in the set showing a negative recovery pattern in the elongation zone, while classes related to the synthesis of eukaryotic (cytosolic) ribosomes were overrepresented among the transcripts with a positive recovery pattern in mature tissue. Functional classes related to protein synthesis, particularly the synthesis of eukaryotic ribosomal proteins, were overrepresented among the transcripts positively correlated to polysome loading and leaf elongation. Functional classes related to the ubiquitin pathway (particularly E3 ligases of the RING type) were overrepresented among the transcripts negatively correlated to polysome loading and leaf elongation and transcripts related to protein degradation by the ubiquitin pathway were *under*represented in the set of transcripts that were positively correlated to polysome loading. Thus, expression of genes involved in protein synthesis and protein degradation changes inversely and in parallel, respectively, with growth. The set of transcripts negatively correlated to Suc concentration shows overrepresentation for amino acid degradation.

We individually reviewed the genes identified by both strategies, particularly those from strategy 2 that correlated with Suc, and prioritizing genes whose annotation

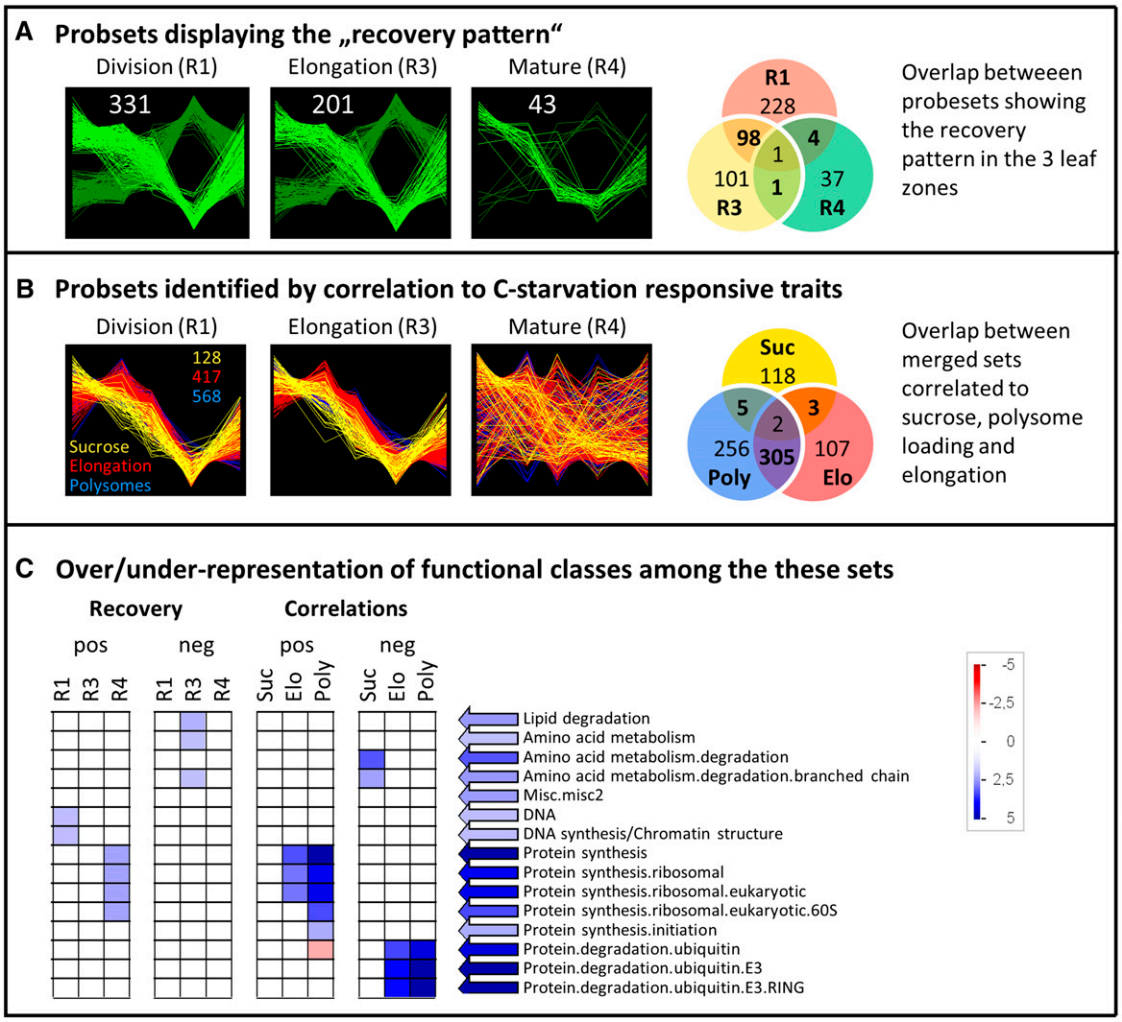

Figure 10. Transcripts identified based on defined pattern over the time course or correlation to target traits. A, Transcripts showing high similarity to the defined "recovery" patterns (see text) in the cell division zone (R1), elongation zone (R3), and mature tissue (R4). The transcripts showing a response pattern similar in orientation to the change in Suc and growth traits (termed "positive") are colored light green, and those showing inverse pattern ("negative") are colored dark green. The Venn diagram shows the overlap between the transcripts showing the recovery pattern in the three leaf regions. B, Transcripts correlated at $R > 0.9$ or $R < -0.9$ to Suc level, polysome loading, or whole-leaf elongation rate over the C starvation time course in any of the correlation approaches described in the text (merged sets). There is thus only one merged set of correlating transcripts per target trait. Here, pattern of the transcripts of these sets are plotted for in each leaf zone, underlining that the identified correlations are mainly driven by the growth zones. The Venn diagram shows the overlap between the merged sets of transcripts correlated to Suc, elongation rate, and polysome loading. C, For the transcripts identified by the recovery pattern or by correlation to target traits (see A, B, and text) ORA for functional classes was conducted with the software Pageman (Usadel et al., 2006), using Fisher test statistics and Benjamini-Hochberg (Benjamini and Hochberg, 1995) multiple testing correction. ORA was separately tested for transcripts displaying positive and negative correlation/pattern. Blue, Overrepresentation; red, underrepresentation.

indicated a regulatory function, such as transcriptional regulation (transcription factors), posttranslational modification, specific protein degradation, signaling, and developmental regulators, as well as C metabolism and transport, and filtered further by examining the reliability of the annotations. The resulting short list (Supplemental Datafile S5) included several protein kinases, among them a MAP pathway kinase (*GRMZM2G400470*), two Leu-rich repeat protein kinases (*GRMZM2G161664*, *GRMZM5G897958*), the SnRK2 family protein kinase *GRMZM2G110908*, the protein kinase *GRMZM2G172900*, which is the ortholog of *AtNEK5* that functions in the regulation of cell expansion via microtubule destabilization (Motose et al., 2012), and *GRMZM5G897958*, which is orthologous to *AtHERK1*, a brassinosteroid responsive receptor kinase required for cell elongation during vegetative growth (Guo et al., 2009a, 2009b), the F-BOX type ubiquitin E3 ligase GRMZM2G151536, orthologous to AtCOI1, which mediates jasmonate responsive protein degradation

(Yan et al., 2009) and the transcription factors *ZmWRKY71*, *ZmALF6*, *ZmEREB182*, *ZmMYB148*, *ZmOrphan151*, *ZmHB58*, *ZmGBP12*, and *ZmbZIP111* (nomenclature according to www.grassius.org). ZmHB58 is orthologous to *ATRev*, which regulates lateral meristem initiation (Otsuga et al., 2001) and has been linked to shade avoidance (Brandt et al., 2012). *ZmbZIP111* is the maize ortholog of Arabidopsis BZIP63, which is part of the Suc responsive BZIP signaling network (Kang et al., 2010) indicating conservation of this sugar responsive network.

Genes with Contrasting Expression Responses between Leaf Regions

We also searched for transcripts that show opposing temporal responses in different leaf zones. To do this, we first identified transcripts with a significant interaction effect and significant time course effects in the individual leaf regions (ANOVA, multiple testing corrected P value < 0.001) and then calculated, for each gene, the Pearson correlation scores between each pair of leaf zones (Supplemental Datafile S4). Over-/underrepresentation analysis (ORA) for functional classes within the sets of transcripts showing a negative correlation (below -0.7, -0.8, or -0.9) between leaf zones did not yield any significant results, indicating a diverse array of transcripts. Manual inspection of these transcripts revealed a short list of 16 candidates (Supplemental Datafile S5). These include several transcription factors, a RING-type E3 ligase, a protein prenyltransferase alpha subunit, whose ortholog *AtFTA* is required for meristem maintenance in Arabidopsis (Running et al., 2004), and a WNK-type Ser/Thr-protein kinase. We also identified some genes involved in C transport and metabolism. The Suc transporter *ZmSUT2/GRMZM2G145107* is initially highest expressed in the growth zones, in line with the observed localization of AtSUT2 and LeSUT2 protein in sink tissues (Meyer et al., 2004; Hackel et al., 2006; Ayre, 2011). During ExN, expression decreases in the growth zones and increases in mature tissue, which exhibits the highest transcript levels at 14hExN. Transcript for *GRMZM2G150796/Isoamylase3* is initially higher in mature tissue but decreases rapidly after onset of the ExN, while it shows a moderate increase from 14hEXN in growth zones. *GRMZM2G040843* (encoding a neutral invertase) is down-regulated in ExN in mature tissue, but up-regulated in the growth zones. These responses point to a readjustment of carbohydrate metabolism and transport in ExN.

DISCUSSION

Marked Gradients of Metabolism and Gene Expression in the Developing Maize Leaf

We have subjected maize to a C starvation treatment, performed metabolite and transcript profiling in the growth and mature zones of leaf 9, and integrated this data with information about growth. In total, we studied 64 metabolites, 11 enzymes, and 3583 transcripts at dusk, at the end of the night and 6, 14, and 24 h into an extended night and related them to whole-leaf elongation and polysome loading, as a proxy for protein synthesis.

There are pronounced differences in metabolic traits (Fig. 2) and expression profiles (Fig. 4) between the leaf zones, with particularly large differences between the growth zones and mature tissue. These developmental gradients affected the majority of the metabolites (Fig. 2) and the vast majority of the transcripts (Supplemental Fig. S5). Our results at dusk are in agreement with previous studies of the transcriptome (Li et al., 2010; Wang et al., 2014), proteome (Majeran et al., 2010), and metabolome (Pick et al., 2011; Wang et al., 2014) of developing maize leaves. While cell division, cell growth, cell expansion, and Suc mobilization, respiration, and anabolic metabolism are predominant at the base of the leaf, there is a gradual but coordinated increase in proteins and metabolites required for the Calvin-Benson cycle and the C4 pathway for CO_2 concentration as the leaf matures. The high levels of malate in the expansion zone have been noted previously by Wang et al. (2014), who proposed that in immature maize leaf tissues, malate acts as a C store or osmoticum, in addition to its role as an intermediate in C4 photosynthesis.

Temporal Response of Carbohydrates, Metabolism, and Gene Expression to Progressive C Depletion Differs between Mature Tissue and Growth Zones

The majority of the metabolites (Fig. 3) and transcripts (Supplemental Fig. S5) showed marked changes during the night and extended night. Although we term this treatment a C-depletion time course, it will include changes due to the circadian clock and the prolonged absence of light; nevertheless, detailed analyses of a similar data series in Arabidopsis showed that C was the major contributor to the changes in global transcript abundance (Bläsing et al., 2005; Usadel et al., 2008).

Analysis of the response of metabolites and transcripts in maize leaves reveals that some general trends are conserved between the leaf zones, such as down-regulation of anabolic processes, up-regulation of catabolism, particularly protein and amino acid degradation, and up-regulation of transcripts for specific protein degradation via the ubiquitin pathway (Figs. 2 and 4). These conserved responses resemble C starvation response in Arabidopsis seedlings and rosettes (Price et al., 2004; Thimm et al., 2004; Osuna et al., 2007; Usadel et al., 2008) and maize roots (Brouquisse et al., 1998). Maize orthologs of several previously described C starvation responsive Arabidopsis genes (*GDH1*, *MIOX1*, *DIN10*) showed a comparable response in our dataset. While a gene encoding Asn synthetase and assigned as the best maize ortholog of *AtAsn1*, a well-described C starvation marker in Arabidopsis (Lam et al., 1994, 1998; Fujiki et al., 2001; Hanson et al., 2008) does not show significant expression change over our time course in

any leaf region, there was a strong accumulation of Asn at 24hExN, indicating that the maize protein is post-transcriptionally activated or that its function is taken over by other orthologs in maize.

Nevertheless, despite some shared trends, maize leaf zones differed considerably in their response during the C-depletion time course. First, the timing and severity of the changes differed between leaf zones, with earlier and more pronounced responses of metabolic traits and transcript abundance in mature tissue than growth zones. Second, Suc (Fig. 3A), other metabolites (Fig. 1, B and C), and many transcripts (Fig. 1, D and E) showed a partial recovery between 14 and 24 h into the extended night in growth zones, but not in mature tissue. Thus, the C starvation response is initiated later, more weakly, and in part transiently in growth zones.

In an Extended Night, Maize Leaf Growth Continues for Several Hours Before It Is Inhibited, and Later Shows a Partial Recovery

When Arabidopsis is subjected to an extended night, polysome loading decreases and growth is inhibited in 1 to 2 h, coinciding with the exhaustion of starch and the onset of C starvation (Gibon et al., 2004b; Yazdanbakhsh et al., 2011; Pal et al., 2013). In contrast, leaf 9 of maize maintained extension growth at the same rate as in the night for 6 h into the extended night (Fig. 5A). The protein content in the growth zones remained unaltered (Supplemental Fig. S2), showing that extension growth was accompanied by protein synthesis. In agreement, polysome loading in the growth zones remained high for the first 6 h of the extended night (Fig. 5B). Extension growth decreased by about 70% between 6 and 14 h into the extended night, and polysome loading also decreased to low values. It should be noted that polysome loading provides a qualitative proxy for protein synthesis but may overestimate protein synthesis rates when polysome loading is low (Pal et al., 2013). From 14 h onwards, there was a small but reproducible increase in the rate of leaf extension. This was accompanied by a slight increase in polysome loading in the cell division but not the extension zone and a decrease in protein content in the growth zones. These observations indicate that extension growth and protein synthesis are synchronously regulated in the first part of the extended night but uncoupled during the partial recovery of growth between 14hEXN and 24hEXN. This may indicate adjustment to C starvation, as protein synthesis is a very costly process (Penning De Vries, 1975). It may also reflect preferential stimulation of cell expansion compared to protein synthesis in darkness.

Leaf Growth Largely Mirrors the Suc Content in the Growth Zones

In the growth zones, the temporal responses of global transcript abundance and polysome loading tracked, with a slight delay, the change in Suc content and showed a similar temporal pattern to whole-leaf elongation rate (Fig. 6A). This contrasts with mature leaf tissues, where Suc and other C metabolites were largely depleted by the end of the night and were unrelated to whole-leaf growth and to Suc levels and polysome loading in the growth zones (Fig. 6B). This indicates that growth is regulated by local C status in the growth zone, rather than by the C status in mature tissue. This underscores the limitations of studies that attempt to relate growth responses to metabolic traits in mature plant tissue or whole rosettes.

The temporal response of whole-leaf elongation and polysome loading is more closely related to Suc content than to the levels of other C metabolites like reducing sugars or organic acids, which do not recover toward the end of the extended night treatment. T6P has been described as a signal of Suc status (Lunn et al., 2006, 2014; Paul et al., 2008; Smeekens et al., 2010; Lastdrager et al., 2014; Yadav et al., 2014). Lunn et al. (2014) proposed a bidirectional relationship in which Suc regulates the level of T6P, and T6P regulates some but probably but not all of pathways that produce and utilize Suc. Interestingly, T6P and Suc showed differing spatial and temporal responses during the C-depletion time course in maize leaves. First, during the undisturbed diurnal cycle (i.e. at dusk and dawn) the T6P:Suc ratio was up to 25-fold higher in the growth zones than in the mature leaf. Second, during the extended night treatment the T6P:Suc ratio in growth zones decreased to a level similar to that in mature tissue. Third, the partial recovery of Suc at after 24 h extended night was not accompanied by an increase in T6P (Figs. 2 and 9). These results extend earlier reports of a high T6P:Suc ratio in tissues with a large demand for Suc including Arabidopsis shoot apical meristems (Wahl et al., 2013) and maize leaf tumors induced by the biotrophic fungus *Ustilago maydis* (Horst et al., 2010). They are consistent with a recent report that T6P correlates with Suc content during the diurnal cycle, but not over a 48 h dark treatment in the mature leaf 3 of maize seedlings (Henry et al., 2014). While it is not known how Suc acts to regulate T6P levels, and how this relationship is developmentally modified in growing tissues, it appears plausible that a high T6P:Suc ratio in growing tissues may promote utilization of Suc, driving Suc levels down and promoting Suc import.

Contrasting Regulation of Starch Reserves in Growth and Mature Zones

The maintenance of Suc levels and continuation of growth of maize leaves during an extended night points to different management of C reserves in maize and the fast-growing dicot weed Arabidopsis. This includes differences in the regulation of starch turnover in growing and mature leaf zones and at the whole-plant scale.

There are striking differences in the management of C reserves in the mature and growth zones of a growing maize leaf. In the mature maize leaf, starch is largely

turned over during the light-dark cycle, with about 20% remaining at dawn (Fig. 3B). This is striking, as the maize plants were grown in a relatively long 14 h photoperiod, which is close to the limit at which Arabidopsis does not completely turn over its starch. The near-complete turnover of starch is in agreement with previous reports for mature maize leaves (Kalt-Torres et al., 1987). In Arabidopsis rosettes, starch degradation is paced by the circadian clock (Graf et al., 2010). A similar mechanism might operate in mature maize leaf tissue. In contrast, starch is not actively degraded during the night in growth zones of maize leaves (Figs. 3B and 8; Supplemental Fig. S3); indeed, continued synthesis may be required to explain how high levels of starch are retained despite dilution by growth (Supplemental Fig. S11). Starch is not degraded in the growth zones until the light-dark cycle is perturbed by extending the night. Further, analyses in whole plants revealed that while the base of older mature leaves contains relatively small amounts of starch, young leaves contain high starch. This starch was also not degraded during the night (Fig. 8). Thus, starch in the growth zones of maize does not function as transitory store to provide C at night, but instead provides a midterm buffer against perturbations that lead to a shortfall of C.

This implies that the clock-based mechanism that couples starch metabolism to the diurnal cycle in mature tissues is either absent or is modified by other factors in the growth zone of a maize leaf. One possibility is that the relatively high levels of Suc in growth zones during the night (Fig. 3A) feedback inhibit starch degradation, and that this inhibition is relieved when Suc levels fall in the extended night. The feedback inhibition might be linked to the very high levels of T6P in the growth zones (Fig. 9A). It was recently shown in Arabidopsis that starch degradation is inhibited by T6P (Martins et al., 2013). It has been proposed that the clock sets the maximal rate of starch degradation, while T6P levels signal the demand for C; when demand is low, Suc and T6P rise and starch breakdown is slowed down (Martins et al., 2013; Lunn et al., 2014). In accordance with this idea, the division zone, which had high T6P level until 14 h into the extended night, also degraded its starch most slowly (compare Figs. 9A and 3B). It is also possible that the clock or clock outputs are modified in growing tissues. For example, the diurnal amplitude of core clock gene transcript levels and the number of clock output genes showing diurnal cycling were strongly reduced in growing maize cobs (Hayes et al., 2010). High Suc levels such were shown to override the clock in Arabidopsis roots (James et al., 2008), and the shoot and root circadian clocks have different rhythmic properties and respond differently to light quality and intensity (Bordage et al., 2016). Support for a potentially decreased role of the clock in the growth zones of monocot leaves comes from the finding that whereas leaf growth is under circadian control in dicots, this is less apparent in monocots (Poiré et al., 2010).

While starch reserves at the base of a growing leaf provide an internal C reserve, our calculations indicate that it covers only a small proportion of the total C that is required for leaf growth during the first 24 h of an extended night (Fig. 7). Furthermore, starch at the base of leaf 9 was largely exhausted by 14 h into the extended night, but Suc levels rose and growth recommenced between 14 and 24 h (compare Fig, 3, Fig. 5A, and Supplemental Fig. S9). This partial recovery presumably depends on C reserves outside leaf 9. While we did not undertake a quantitative analysis, our results indicate that there are considerable reserves of starch in the stem tissue, older leaves, and leaf nodes of old and young leaves, which are remobilized to support the growth of young leaves during an extended night (Fig. 8). The leaf nodes adjacent to the youngest leaves retained starch for longest into the extended night, indicating that very young leaves are prioritized in C starvation.

Midterm C reserves could have several functions. They may buffer maize against perturbations in the environment that lead to a shortfall in C and disturbance of growth. By facilitating a partial recovery of leaf growth and in particular extension growth in extended darkness, they may also support a growth response to extreme shading. Starch reserves in the leaf bases and stems may also support rapid regrowth after grazing; while this may not be a major consideration for field-grown maize, it may be more relevant for related wild species. It is also possible that the higher rate of photosynthesis in the C4 species maize and the relatively long photoperiod used in our experiments provide more C for growth than was available in many of the studies of starch turnover in dicots. Indeed, C reserves also accumulate in Arabidopsis when it is grown in high irradiance and long photoperiods (Hädrich et al., 2011; Lauxmann et al., 2016; Pilkington et al., 2015).

Identification of Candidate Genes Based on the Temporal Expression Pattern or Contrasting Expression Pattern in Growing and Mature Leaf Zones

The overall spatiotemporal changes in gene expression in the growth zones over the C-starvation time course shows a similar pattern to that of the Suc content and polysome loading in the growth zones, and the whole-leaf elongation rate (Fig. 6). This indicates that many of the changes in expression occur in a coordinated manner with the changes in growth and could be directly or indirectly related to changes in Suc levels. We used two strategies to identify functional classes and individual genes with a similar response to that of Suc and growth. In one, we filtered for genes with a qualitatively similar response patterns, in particular the partial recovery between 14ExN and 24hExN. Overrepresentation analysis of transcripts showing the recovery pattern revealed overenrichment for DNA-synthesis-related transcripts in the cell division zone, and for protein-synthesis-related transcripts in the mature tissue. In the second, we searched for transcripts whose abundance correlated to Suc, leaf elongation, or polysome loading. Since there is a temporal shift between the changes of Suc and the growth traits, this approach distinguished between early (Suc coregulated) and late (growth traits coregulated) responding transcripts.

Overrepresentation analysis revealed a correlation between Suc depletion and the induction of amino acid degradation, while protein synthesis and degradation correlated more closely with growth traits. We also used the individual transcripts identified by both approaches to assemble a shortlist of candidate genes that may have key regulatory functions (Supplemental Datafile S5). This list contains several protein kinases and transcription factors, some orthologous on the protein level to Arabidopsis proteins that have been previously characterized in the context of cell expansion growth, meristematic function, and/or phytohormone signaling, while others have not been closely characterized so far (see results chapter, Supplemental Datafile S5). *ZmBZIP111* is an ortholog of *AtBZIP63*, which is involved in C signaling in Arabidopsis, indicating conservation in C signaling pathways. Others have not or so far only have indirectly been implicated in C signaling. We also searched for transcripts with strongly contrasting transcriptional responses in growth zones and mature tissue (Supplemental Datafile S5). While we did not find any overrepresented functional classes, we identified several potential regulatory proteins, and some genes involved in carbohydrate transport and metabolism, which may have a role in readjusting C distribution and usage within the leaf under C starvation.

In summary, young maize plants contain significant C reserves, including starch at the leaf base and in the adjoining stem. Starch is nearly exhausted by the end of the night in mature leaf tissue, and an extension of the night leads to C starvation, as seen in Arabidopsis. However, in growth zones, reserves buffer metabolism, gene expression, and growth against a temporary shortfall in C and allow partial recovery of Suc levels and resumption of growth in extended darkness. Growth, monitored as polysome loading in individual zones or whole-leaf extension, correlates strongly with Suc levels in the cell division and extension zones, but not with Suc or starch reserves in the mature leaf tissue. This emphasizes that spatially resolved analyses of metabolism and gene expression are vital for studies of the molecular basis of growth and for understanding varying strategies for resource allocation and use among species, organs, and developmental stages. Deeper elucidation of the mechanisms how plants, particularly crop species, deal with C limitation on the spatiotemporal level will be important for further crop improvement. Future studies will need to take into account additional factors, including the balance between different cell types within the leaf regions (Stitt and Heldt, 1985; Pollock et al., 2003; Majeran et al., 2005) and subcellular compartmentation of metabolism (Sweetlove and Fernie, 2013; Tiessen and Padilla-Chacon, 2013).

MATERIALS AND METHODS

Chemicals

Chemicals and enzymes were obtained from Merck, Sigma, and Roche, and from other established providers of substances for laboratory use. Cycloheximide, chloramphenicol, and heparin were obtained from Carl Roth GmbH. If not otherwise stated, all solutions were prepared with purified deionized water (PureLab plus; ELGA LabWater).

Plant Growth

Maize (*Zea mays*) genotype SL (KWS Saatgut AG) was grown in a walk-in growth chamber at the MPI-MP Golm. Plants were grown at 700 μE photosynthetically active radiation, 14 h light/10 h dark cycles, temperature settings 25°C/22°C (the effective day temperature at the plant level is ~29°C), 70% air humidity. At the switches between light and dark periods, the light batteries of the chamber were successively turned on/off during a 30/40 min dawn/dusk period. This measure is necessary to allow a stable behavior of the temperature and air humidity controls in the chamber (the lamps cause significant amounts of heat and water evaporation, and the chamber has a large air volume). To further stabilize air humidity during the light period, water-soaked fleece tissue was spread across parts of the chamber floor. Three-centimeter-thick Styrofoam plates were put below plant pots to isolate them against heating of the metallic chamber floor in the light.

Sampling

Plants were grown to approximately 3.5 weeks of age, when leaf 9 was in the stage of rapid blade elongation and the mature (dark green) leaf tip was sufficiently exposed for connecting it to the elongation measurement apparatus (typically the third day after leaf emergence from the whirl). Four zones of the leaf (see Fig. 1A) were sampled at five time points before and during an extended night. Zone 1 was taken directly above the preligula band and zones 2 and 3 directly next to zone 1, each 1.5 cm length. Zone 4 (mature tissue) was taken 5 cm inward from the leaf tip. Samples were instantly frozen in liquid nitrogen. For each time point and leaf region, three replicates were sampled successively, each replicate pooled from five leaves. For sampling in the dark, a green lamp that emits no photosynthetically active radiation was used. Dissection at the last time point (24hExN) confirmed that the sampled leaves were still at the stage of rapid blade elongation up to the end of the time course. Frozen leaf material was ground to a fine powder at −60°C using a cryogenic grinding robot (Labman) available at the MPI-MP.

Maize Leaf Cell Length Profile and Determination of Percent Dividing Nuclei across the Leaf

Cell length profile determination and cell division analyses were based on the methodology described by Rymen et al. (2010) and Nelissen et al. (2013) with a few modifications indicated below. Plants were grown as stated above and sampled during the day (early afternoon). For cell length profile determination, samples were taken from the preligular band up to 10 cm above. Samples were initially fixed in ethanol then cleared in lactic acid and then washed with phosphate-buffered saline and stained by propidium iodine, which stains plant cell walls (2 h-o/n). Samples were then cut into two halves (each 5 cm long) and from each half, the midvein was removed, and one side of the leaf was embedded in lactic acid for microscopy. From each microscopic slide, an area covering the whole length of the sample and, in width, at least two to three complete intervein sections, was recoding at 20× magnification using a Spinning Disk Confocal UltraView VoX Axio Observer microscope with autostich feature. Both the DIC transmitted light channel and red fluorescent channel (which visualized propidium iodine) were recorded at three z-positions to ensure a good focus on the epidermal layer across the sample. For cell length evaluation, Fiji software was used (Schindelin et al., 2012). At positions approximately every 4 mm along the leaf, typically 20 to 40 cells were measured from at least four separate cell files. Cell files next to stomatal rows were measured. In the R statistical environment, median cell length at each position was calculated, and the cumulative datapoints from 4four replicate leaves were used to fit a second-degree polynomial function by the locpoly function from the R package (R Development Core Team, 2011) KernSmooth (Wand and Jones, 1995). The x intercepts of the first derivative of this function indicate the start and end of the cell elongation zone. For visualization of dividing nuclei, samples were fixed in 3:1 EtOH:acetic acid, washed in phosphate-buffered saline, and stained by 4′,6-diamino-phenylindole (2–3 min). At 3 mm intervals, percent of dividing nuclei in relation to all nuclei in the epidermal cell layer was determined within a predefined area, which typically covered 300 to 700 nuclei.

Leaf Elongation Measurement

Leaf 9 (or in the replicate experiment, leaf 8) at the stage of rapid blade elongation was measured once the leaf tip was sufficiently exposed (see above). Elongation measurement for leaf 8 was performed during the same experiment

when samples were taken for 10 randomly chosen plants of the same culture. The principle of the RRT-based measurement of elongation rate is visualized and explained in Supplemental Figure S9A.

Determination of Metabolite Level, Enzyme Activity, Polysome Loading, and Expression Profiles

Starch, Glc, Fru, Suc, malate, fumarate, Glc-6-phosphate, nitrate, chlorophyll *a* and *b*, total amino acid content, and total protein content were determined from ethanolic extracts of approximately 20 mg of leaf powder or from the precipitate of this extraction (starch, protein) by previously described assays using an established, semirobotized determination platform (Cross et al., 2006). Enzyme activity measurements were conducted as previously described by Gibon et al. (2004a) and Sulpice et al. (2010) using an established semirobotized 96-well microtiter plate platform. Gas chromatography-mass spectrometry metabolite measurements were conducted as described (Tohge et al., 2011). Liquid chromatography-mass spectrometry-based metabolite measurement, including measurement of T6P, was conducted as described by Lunn et al. (2006).

Polysome loading was determined as described by Piques et al. (2009). Other than in Piques et al. (2009), we only differentiated in evaluation between the nonpolysome peak (i.e. free ribosomes) and the polysome peak (i.e. transcripts loaded with ribosomes). Instead of 100 mg of plant tissue fresh weight, only 40 mg were used, since the sampled material from the carbon starvation experiments was limited.

For transcript profiling, total RNA from maize leaf tissue was extracted with the RNeasy Plant Mini Kit (Qiagen) according to the manufacturer's manual. Instead of β-mercaptoethanol, dithiothreitol was used in the extraction buffer. RNA concentration and quality were determined with a Nanodrop Microvolume UV-Vis spectrometer (Thermo-Fisher Scientific) and with the Agilent Bioanalyzer using the "RNA Nano chip" (Agilent). Based on the concentrations determined by the Nanodrop, each sample was diluted to a concentration of 350 μg RNA/mL. Three hundred microliters of this dilution was sent to ATLAS Biolabs for Affymetrix maize gene chip gene expression array hybridization.

Iodine Staining

Samples for iodine staining stored in 100% ethanol at −20°C until further processing. Samples were then destained in 100% ethanol at 95°C for approximately 2 h until all chlorophyll was removed and the samples were pale yellow. Ethanol was exchanged in between. Subsequently, the samples were resuspended in deionized water for 10 min at room temperature and then stained with Lugol's solution (8 mM I2, 300 mM KI) for 5 min (light protected), washed in water two times, and then arranged for photographing.

Gas Exchange Measurement

Gas exchange was measured with the "portable photosynthesis system HCM-1000" apparatus from Heinz Waltz GmbH using a cuvette that covered 2 cm^2 of mature leaf area. Gas exchange was measured for a single plant from the same culture during the extended night time course. Measurement points were recorded every 10 min. For each measurement point, the net photosynthesis rate (μmol CO_2 m^{-2} s^{-1}) was calculated by the system-specific software (version 1.01). A total area of 14.5 cm^2 mature leaf tissue was assumed based on iodine staining. To convert μmol CO_2 to mg Glc equivalent units, the values were divided by 6 (6 carbon units per Glc) and then multiplied by the molar weight of Glc/1000. Calculations: Supplemental Datafile S3.

Calculations, Statistical Analyses, and Plotting

The statistical environment R, version 3.0.1, Sigma Plot 12.5 (Systat Software) or MS Excel 2010 (Microsoft) were used for analyses and plotting of figures, unless otherwise stated.

Normalization of Metabolomic Dataset and Calculation of Mean Metabolic Change Relative to ED

For visualization of the metabolomic dataset by PCA, calculation of mean metabolic change relative to ED, and hierarchical clustering of metabolic traits, the measured metabolite values for each trait were converted to *z*-scores. To do this, the following formula was applied, for each trait i, leaf region l, time point t,:

$$\text{trait\_zscore}_{i,l,t} = (\text{trait\_raw}_{i,l,t}\text{-mean}(\text{trait\_raw}_i))/\text{standard\_deviation}(\text{trait\_raw}_i)$$

This conversion adjusts the distribution of measured values for each trait so that the mean of all measured values is zero and the SD is 1, therefore giving equal weight to all metabolic traits in the subsequent analyses. Mean metabolic change to ED for each leaf region l and time point t was calculated as follows:

$$\text{Mean\_Change\_to\_ED}_{l,t} = \sum_1^n Abs(\text{trait\_zscore}_{i,l,t}\text{-trait\_zscore}_{i,l,ED})/n$$

n, number of all metabolic traits; ED, end of day time point.

Calculation of Starch Dilution by Growth

The term "starch dilution by growth" refers to the theoretical change in starch content in the growth zones due to tissue elongation, under the assumptions that starch is neither synthesized nor degraded during an interval and is equally distributed over the tissue during elongation. We estimated this for the summed starch content in the transition and the elongation zones (R2 and R3, i.e. 1.5 cm–4.5 cm above the ligule), since no elongation was observed in the cell division zone R1 (the first 1.5 cm of the leaf; see Supplemental Fig. S1B). Based on our cell length profile across the leaf (Supplemental Fig. S1B), the assumption that this region accounts for 50% of whole-leaf elongation occurs was used. The following formula was used to estimate starch dilution by growth at 5 min resolution (the resolution of the elongation data):

$$\text{Starch}_{t1} = \text{Starch}_{t0} \times \text{length}_{\text{sampled growth zone}} \Big/ \left(\text{length}_{\text{sampled growth zone}} + 0.5 \times \text{elongation}_{t0 \to t1}\right)$$

t0/t1, time point 0/1; details of this calculation are also given in Supplemental Datafile S3. An explanatory visualization is provided in Supplemental Figure S11A.

Calculation of the Balance between Carbon Requirements for Growth and Available Leaf Carbon Resources

We calculated the required amount of C substrate for the observed leaf elongation growth during the C starvation experiment based on the calculation by Penning De Vries (1975) that 1.055 g of Suc are needed as carbon source for the synthesis of 1 g mixed organic matter (dry weight). 1.055 g of Suc corresponds to 1.11 g of Glc units based on the M_r of two Glc molecules (or one Glc and one Fru molecule) compared to Suc. The M_r of one Glc molecule was equally used to convert the carbohydrate content in the sampled 4.5 cm of the growth zone (sum of Glc, Fru, Suc, and starch as μmol Glc units) into grams. Leaf elongation growth per time interval was calculated from our leaf elongation measurements. Based on dry weight determination of the sampled growth regions at the end of the night, we calculate how much dry weight has to be synthesized for a certain length of leaf elongation. When calculating reduction of carbon reserves between two subsequent time points, carbohydrate reserves (starch, Suc, Glc, Fru) and other C sources (malate, fumarate, amino acids) were separately accounted for. To calculate C release from carbon reserves in the mature leaf part, the sampled zone of the mature leaf was used to extrapolate to the assumed total area of mature leaf tissue based on iodine staining. We also calculated the estimated amount of carbon respired during the time interval in the mature leaf area based on gas exchange. All calculations are given in Supplemental Datafile S3.

Processing of Affymetrix Expression Dataset

Affymetrix gene expression values were normalized by the Robust multi-arrays average algorithm using the software Robin (Lohse et al., 2010). Three samples (one replicate from leaf region 3 time point 1, one replicate from region 4 time point 1, and one replicate from region 4 time point 3) were excluded from further analysis based on atypical behavior in the Robin quality controls.

The dataset was filtered to retain only probesets where at least nine of 11 probes match, with maximum of two mismatches per maize gene model (genome release ZmB73_5b) and which match only to one gene model. In cases where two or more probesets matched to the same gene model, only the highest expressed was retained. Only 3583 passed these filters. For these probesets, a new Mapman (Thimm et al., 2004) based on Mercator (Lohse et al., 2014) mapping for the maize genome release Zm_B73_5b was assembled. In some cases (transcripts discussed in the text), annotation was manually checked and improved. Annotation for the 3583 retained probesets is contained in Supplemental Datafile S4.

Strategies to Identify Transcripts with Characteristic Response Patterns over the Time Course or Contrasting Response between the Leaf Regions and Selection of Shortlists

Identification of transcripts that display a characteristic response pattern over the carbon starvation time course was conducted by using an R-script that applies consecutive filtering steps upon the transcripts (mean values of three Affymetrix arrays), so that in the end only transcripts that fulfill all requirements are retained. Filters used were (1) significant expression change over the time course (ANOVA, Benjamini-Hochberg corrected P value < 0.01), (2) significant difference in transcript abundance between ED and 14hEXN time points ≥70% of maximum difference between any time points, and (3) significant difference in transcript abundance between 14hExN and 24hEXN time points ≥15% of maximum difference between any time points. Direction of change has to be reversed between the ED-14hExN interval and the 14hEXN-24hEXN. Patterns with strong outliers or circadian-type patterns were excluded.

Correlations between transcript patterns and Suc level, leaf elongation rate, and polysome loading were determined by Spearman correlation, multiple testing correction by the Benjamini-Hochberg method. Either (a) a vector of the unmodified expression values in division+elongation zone or all three leaf zones was correlated against a vector of the trait values in the same zones, or (b) the expression or trait values in each individual zone were first normalized to their mean and SD (z-score), and these normalized values for each zone were used as a basis to build up vectors for the correlation tests as described for approach (a).

Transcripts with contrasting expression pattern between leaf zones were identified by Pearson correlation between expression vectors of two zones (e.g. division zone versus mature zone expression values) and selecting those with highly negative correlation between zones.

Accession Numbers

Affymetrix Probeset IDs and GRMZM maize gene model identifiers for all analyzed transcripts are given in Supplemental Datafile S4.

Supplemental Data

The following supplemental materials are available:

Supplemental Figure S1. Identification of cell division and cell expansion zones by analysis of nucleus size and microscopic analysis of the percentage of dividing cells and cell length.

Supplemental Figure S2. Measurement of total protein concentration in four leaf zones at five time points over the ExN time course.

Supplemental Figure S3. Starch staining of maize leaves sampled over the carbon starvation time course.

Supplemental Figure S4. Comparison of the overall pattern of change in gene expression over the C starvation time course between division zone, elongation zone, and mature tissue of the growing maize leaf blade.

Supplemental Figure S5. Venn diagram of transcripts that show significant expression changes between the maize leaf developmental zones and/or upon carbon starvation.

Supplemental Figure S6. Gene expression differences between three zones of the growing maize leaf blade at five time points of a C starvation time course—ORA for functional classes.

Supplemental Figure S7. Comparison of gene expression responses and metabolic/enzymatic responses for Glu dehydrogenase and myoinositol/myoinositol oxygenase.

Supplemental Figure S8. Expression of genes of interest in three leaf zones of the growing maize leaf blade across the C starvation time course—C signaling and orthologs of described C starvation markers.

Supplemental Figure S9. Determination of growth-related traits over the C starvation time course.

Supplemental Figure S10. Overlay of the responses of different traits to a C starvation time course in the elongation zone of the growing maize leaf blade.

Supplemental Figure S11. Starch dilution by growth.

Supplemental Figure S12. Changes in maltose level over the C starvation time course.

Supplemental Figure S13. Gas exchange measurement.

Supplemental Datafile S1. Data table with mean and SD for all metabolic traits.

Supplemental Datafile S2. Plots for all individual metabolic traits.

Supplemental Datafile S3. Dilution of starch by growth and relation between C reserves and C requirements of growth in leaf 9: calculations and data (fresh weight, dry weight, metabolites, photosynthesis, respiration).

Supplemental Datafile S4. Robust multiarrays average normalized gene expression data for all probesets of the filtered Affymetrix dataset, annotation, results of pattern classification, correlation to Suc, elongation rate, polysome loading, and correlation of expression values between leaf regions for each probeset.

Supplemental Datafile S5. Shortlist of genes of interest selected based on their transcript abundance over the time course or contrasting transcript pattern between leaf zones, in combination with annotation and literature on orthologs in other species.

ACKNOWLEDGMENTS

We thank Armin Schlereth, Vanessa Wahl, and Eva-Theresa Pyl for discussions, Maria Piques and Sunil Kumar Pal for sharing their protocol and instructions for polysome loading analysis, Christin Abel and Didi-Andreas Song for help with sampling and analysis, respectively, of samples for cell length and cell division profile analysis, Marek Szechowka for reanalysis of maltose peaks in the gas chromatography-mass spectrometry profiles, Björn Usadel and Federico Giorgi for statistical advice, the Max Planck Institute of Molecular Plant Physiology greenhouse team led by Karin Köhl, particularly Helga Kulka and Britta Hausmann, for taking care of our plants, and Andre Germann and Toralf Eifrig for technical help.

Received June 23, 2016; accepted August 26, 2016; published August 31, 2016.

LITERATURE CITED

Alford SR, Rangarajan P, Williams P, Gillaspy GE (2012) myo-Inositol oxygenase is required for responses to low energy conditions in Arabidopsis thaliana. Front Plant Sci **3:** 69

Andriankaja M, Dhondt S, De Bodt S, Vanhaeren H, Coppens F, De Milde L, Mühlenbock P, Skirycz A, Gonzalez N, Beemster GTS, et al (2012) Exit from proliferation during leaf development in Arabidopsis thaliana: a not-so-gradual process. Dev Cell **22:** 64–78

Apelt F, Breuer D, Nikoloski Z, Stitt M, Kragler F (2015) Phytotyping(4D) : a light-field imaging system for non-invasive and accurate monitoring of spatio-temporal plant growth. Plant J **82:** 693–706

Avramova V, AbdElgawad H, Zhang Z, Fotschki B, Casadevall R, Vergauwen L, Knapen D, Taleisnik E, Guisez Y, Asard H, et al (2015a) Drought induces distinct growth response, protection, and recovery mechanisms in the maize leaf growth zone. Plant Physiol **169:** 1382–1396

Avramova V, Sprangers K, Beemster GT (2015b) The maize leaf: another perspective on growth regulation. Trends Plant Sci **20:** 787–797

Ayre BG (2011) Membrane-transport systems for sucrose in relation to whole-plant carbon partitioning. Mol Plant **4:** 377–394

Baena-González E, Rolland F, Thevelein JM, Sheen J (2007) A central integrator of transcription networks in plant stress and energy signalling. Nature **448:** 938–942

Ben-Haj-Salah H, Tardieu F (1995) Temperature affects expansion rate of maize leaves without change in spatial distribution of cell length (analysis of the coordination between cell division and cell expansion). Plant Physiol **109:** 861–870

Benjamini Y, Hochberg Y (1995) Controlling the false discovery rate—a practical and powerful approach to multiple testing. J R Stat Soc Series B Stat Methodol **57:** 289–300

Bläsing OE, Gibon Y, Günther M, Höhne M, Morcuende R, Osuna D, Thimm O, Usadel B, Scheible WR, Stitt M (2005) Sugars and circadian

regulation make major contributions to the global regulation of diurnal gene expression in Arabidopsis. Plant Cell **17:** 3257–3281

Bordage S, Sullivan S, Laird J, Millar AJ, Nimmo HG (2016) Organ specificity in the plant circadian system is explained by different light inputs to the shoot and root clocks. New Phytol **212:** 136–149

Brandt R, Salla-Martret M, Bou-Torrent J, Musielak T, Stahl M, Lanz C, Ott F, Schmid M, Greb T, Schwarz M, et al (2012) Genome-wide binding-site analysis of REVOLUTA reveals a link between leaf patterning and light-mediated growth responses. Plant J **72:** 31–42

Brouquisse R, Gaudillere JP, Raymond P (1998) Induction of a carbon-starvation-related proteolysis in whole maize plants submitted to light/dark cycles and to extended darkness. Plant Physiol **117:** 1281–1291

Brouquisse R, James F, Pradet A, Raymond P (1992) Asparagine metabolism and nitrogen distribution during protein degradation in sugar-starved maize root tips. Planta **188:** 384–395

Cho YH, Yoo SD, Sheen J (2006) Regulatory functions of nuclear hexokinase1 complex in glucose signaling. Cell **127:** 579–589

Cross JM, von Korff M, Altmann T, Bartzetko L, Sulpice R, Gibon Y, Palacios N, Stitt M (2006) Variation of enzyme activities and metabolite levels in 24 Arabidopsis accessions growing in carbon-limited conditions. Plant Physiol **142:** 1574–1588

Deprost D, Yao L, Sormani R, Moreau M, Leterreux G, Nicolaï M, Bedu M, Robaglia C, Meyer C (2007) The Arabidopsis TOR kinase links plant growth, yield, stress resistance and mRNA translation. EMBO Rep **8:** 864–870

Devaux C, Baldet P, Joubès J, Dieuaide-Noubhani M, Just D, Chevalier C, Raymond P (2003) Physiological, biochemical and molecular analysis of sugar-starvation responses in tomato roots. J Exp Bot **54:** 1143–1151

Dolezel J, Greilhuber J, Suda J (2007) Estimation of nuclear DNA content in plants using flow cytometry. Nat Protoc **2:** 2233–2244

Dong XF, Cui N, Wang L, Zhao XC, Qu B, Li TL, Zhang GL (2012) The SnRK protein kinase family and the function of SnRK1 protein kinase. Int J Agr Biol **14:** 575–579

Facette MR, Shen Z, Björnsdóttir FR, Briggs SP, Smith LG (2013) Parallel proteomic and phosphoproteomic analyses of successive stages of maize leaf development. Plant Cell **25:** 2798–2812

Figueroa CM, Feil R, Ishihara H, Watanabe M, Kölling K, Krause U, Höhne M, Encke B, Plaxton WC, Zeeman SC, et al (2016) Trehalose 6-phosphate coordinates organic and amino acid metabolism with carbon availability. Plant J **85:** 410–423

Fujiki Y, Yoshikawa Y, Sato T, Inada N, Ito M, Nishida I, Watanabe A (2001) Dark-inducible genes from Arabidopsis thaliana are associated with leaf senescence and repressed by sugars. Physiol Plant **111:** 345–352

Gibon Y, Blaesing OE, Hannemann J, Carillo P, Höhne M, Hendriks JHM, Palacios N, Cross J, Selbig J, Stitt M (2004a) A Robot-based platform to measure multiple enzyme activities in Arabidopsis using a set of cycling assays: comparison of changes of enzyme activities and transcript levels during diurnal cycles and in prolonged darkness. Plant Cell **16:** 3304–3325

Gibon Y, Bläsing OE, Palacios-Rojas N, Pankovic D, Hendriks JHM, Fisahn J, Höhne M, Günther M, Stitt M (2004b) Adjustment of diurnal starch turnover to short days: depletion of sugar during the night leads to a temporary inhibition of carbohydrate utilization, accumulation of sugars and post-translational activation of ADP-glucose pyrophosphorylase in the following light period. Plant J **39:** 847–862

Gibon Y, Pyl ET, Sulpice R, Lunn JE, Höhne M, Günther M, Stitt M (2009) Adjustment of growth, starch turnover, protein content and central metabolism to a decrease of the carbon supply when Arabidopsis is grown in very short photoperiods. Plant Cell Environ **32:** 859–874

Gibon Y, Usadel B, Blaesing OE, Kamlage B, Hoehne M, Trethewey R, Stitt M (2006) Integration of metabolite with transcript and enzyme activity profiling during diurnal cycles in Arabidopsis rosettes. Genome Biol **7:** R76

Gonzalez N, Vanhaeren H, Inzé D (2012) Leaf size control: complex coordination of cell division and expansion. Trends Plant Sci **17:** 332–340

Graf A, Schlereth A, Stitt M, Smith AM (2010) Circadian control of carbohydrate availability for growth in Arabidopsis plants at night. Proc Natl Acad Sci USA **107:** 9458–9463

Graf A, Smith AM (2011) Starch and the clock: the dark side of plant productivity. Trends Plant Sci **16:** 169–175

Granot D, David-Schwartz R, Kelly G (2013) Hexose kinases and their role in sugar-sensing and plant development. Front Plant Sci **4:** 44

Guo H, Li L, Ye H, Yu X, Algreen A, Yin Y (2009a) Three related receptor-like kinases are required for optimal cell elongation in Arabidopsis thaliana. Proc Natl Acad Sci USA **106:** 7648–7653

Guo H, Ye H, Li L, Yin Y (2009b) A family of receptor-like kinases are regulated by BES1 and involved in plant growth in Arabidopsis thaliana. Plant Signal Behav **4:** 784–786

Hackel A, Schauer N, Carrari F, Fernie AR, Grimm B, Kühn C (2006) Sucrose transporter LeSUT1 and LeSUT2 inhibition affects tomato fruit development in different ways. Plant J **45:** 180–192

Hädrich N, Gibon Y, Schudoma C, Altmann T, Lunn JE, Stitt M (2011) Use of TILLING and robotised enzyme assays to generate an allelic series of Arabidopsis thaliana mutants with altered ADP-glucose pyrophosphorylase activity. J Plant Physiol **168:** 1395–1405

Halford NG, Hey SJ (2009) Snf1-related protein kinases (SnRKs) act within an intricate network that links metabolic and stress signalling in plants. Biochem J **419:** 247–259

Hanson J, Hanssen M, Wiese A, Hendriks MM, Smeekens S (2008) The sucrose regulated transcription factor bZIP11 affects amino acid metabolism by regulating the expression of ASPARAGINE SYNTHETASE1 and PROLINE DEHYDROGENASE2. Plant J **53:** 935–949

Hayes KR, Beatty M, Meng X, Simmons CR, Habben JE, Danilevskaya ON (2010) Maize global transcriptomics reveals pervasive leaf diurnal rhythms but rhythms in developing ears are largely limited to the core oscillator. PLoS One **5:** e12887

Henry C, Bledsoe SW, Siekman A, Kollman A, Waters BM, Feil R, Stitt M, Lagrimini LM (2014) The trehalose pathway in maize: conservation and gene regulation in response to the diurnal cycle and extended darkness. J Exp Bot **65:** 5959–5973

Honig A, Avin-Wittenberg T, Ufaz S, Galili G (2012) A new type of compartment, defined by plant-specific Atg8-interacting proteins, is induced upon exposure of Arabidopsis plants to carbon starvation. Plant Cell **24:** 288–303

Horst RJ, Doehlemann G, Wahl R, Hofmann J, Schmiedl A, Kahmann R, Kämper J, Sonnewald U, Voll LM (2010) Ustilago maydis infection strongly alters organic nitrogen allocation in maize and stimulates productivity of systemic source leaves. Plant Physiol **152:** 293–308

Ingram GC, Waites R (2006) Keeping it together: co-ordinating plant growth. Curr Opin Plant Biol **9:** 12–20

Ishihara H, Obata T, Sulpice R, Fernie AR, Stitt M (2015) Quantifying protein synthesis and degradation in Arabidopsis by dynamic 13CO2 labeling and analysis of enrichment in individual amino acids in their free pools and in protein. Plant Physiol **168:** 74–93

Izumi M, Wada S, Makino A, Ishida H (2010) The autophagic degradation of chloroplasts via rubisco-containing bodies is specifically linked to leaf carbon status but not nitrogen status in Arabidopsis. Plant Physiol **154:** 1196–1209

James AB, Monreal JA, Nimmo GA, Kelly CL, Herzyk P, Jenkins GI, Nimmo HG (2008) The circadian clock in Arabidopsis roots is a simplified slave version of the clock in shoots. Science **322:** 1832–1835

Jang JC, Sheen J (1994) Sugar sensing in higher plants. Plant Cell **6:** 1665–1679

Kalt-Torres W, Kerr PS, Usuda H, Huber SC (1987) Diurnal changes in maize leaf photosynthesis : I. Carbon exchange rate, assimilate export rate, and enzyme activities. Plant Physiol **83:** 283–288

Kang SG, Price J, Lin PC, Hong JC, Jang JC (2010) The arabidopsis bZIP1 transcription factor is involved in sugar signaling, protein networking, and DNA binding. Mol Plant **3:** 361–373

Kawaguchi R, Williams AJ, Bray EA, Bailey-Serres J (2003) Water-deficit-induced translational control in Nicotiana tabacum. Plant Cell Environ **26:** 221–229

Kim B-H, von Arnim AG (2006) The early dark-response in Arabidopsis thaliana revealed by cDNA microarray analysis. Plant Mol Biol **60:** 321–342

Kim YM, Heinzel N, Giese JO, Koeber J, Melzer M, Rutten T, Von Wirén N, Sonnewald U, Hajirezaei MR (2013) A dual role of tobacco hexokinase 1 in primary metabolism and sugar sensing. Plant Cell Environ **36:** 1311–1327

Lam H-M, Hsieh M-H, Coruzzi G (1998) Reciprocal regulation of distinct asparagine synthetase genes by light and metabolites in Arabidopsis thaliana. Plant J **16:** 345–353

Lam HM, Peng SSY, Coruzzi GM (1994) Metabolic regulation of the gene encoding glutamine-dependent asparagine synthetase in Arabidopsis thaliana. Plant Physiol **106:** 1347–1357

Lastdrager J, Hanson J, Smeekens S (2014) Sugar signals and the control of plant growth and development. J Exp Bot **65:** 799–807

Lauxmann MA, Annunziata MG, Brunoud G, Wahl V, Koczut A, Burgos A, Olas JJ, Maximova E, Abel C, Schlereth A, et al (2016) Reproductive failure in Arabidopsis thaliana under transient carbohydrate limitation:

flowers and very young siliques are jettisoned and the meristem is maintained to allow successful resumption of reproductive growth. Plant Cell Environ **39:** 745–767

Lawlor DW, Paul MJ (2014) Source/sink interactions underpin crop yield: the case for trehalose 6-phosphate/SnRK1 in improvement of wheat. Front Plant Sci **5:** 418

Li L, Stoeckert CJ Jr, Roos DS (2003) OrthoMCL: identification of ortholog groups for eukaryotic genomes. Genome Res **13:** 2178–2189

Li P, Ponnala L, Gandotra N, Wang L, Si Y, Tausta SL, Kebrom TH, Provart N, Patel R, Myers CR, et al (2010) The developmental dynamics of the maize leaf transcriptome. Nat Genet **42:** 1060–1067

Lohse M, Nagel A, Herter T, May P, Schroda M, Zrenner R, Tohge T, Fernie AR, Stitt M, Usadel B (2014) Mercator: a fast and simple web server for genome scale functional annotation of plant sequence data. Plant Cell Environ **37:** 1250–1258

Lohse M, Nunes-Nesi A, Krüger P, Nagel A, Hannemann J, Giorgi FM, Childs L, Osorio S, Walther D, Selbig J, et al (2010) Robin: an intuitive wizard application for R-based expression microarray quality assessment and analysis. Plant Physiol **153:** 642–651

Lunn JE, Delorge I, Figueroa CM, Van Dijck P, Stitt M (2014) Trehalose metabolism in plants. Plant J **79:** 544–567

Lunn JE, Feil R, Hendriks JHM, Gibon Y, Morcuende R, Osuna D, Scheible WR, Carillo P, Hajirezaei MR, Stitt M (2006) Sugar-induced increases in trehalose 6-phosphate are correlated with redox activation of ADPglucose pyrophosphorylase and higher rates of starch synthesis in Arabidopsis thaliana. Biochem J **397:** 139–148

Ma J, Hanssen M, Lundgren K, Hernández L, Delatte T, Ehlert A, Liu C-M, Schluepmann H, Dröge-Laser W, Moritz T, et al (2011) The sucrose-regulated Arabidopsis transcription factor bZIP11 reprograms metabolism and regulates trehalose metabolism. New Phytol **191:** 733–745

Majeran W, Cai Y, Sun Q, van Wijk KJ (2005) Functional differentiation of bundle sheath and mesophyll maize chloroplasts determined by comparative proteomics. Plant Cell **17:** 3111–3140

Majeran W, Friso G, Ponnala L, Connolly B, Huang M, Reidel E, Zhang C, Asakura Y, Bhuiyan NH, Sun Q, et al (2010) Structural and metabolic transitions of C4 leaf development and differentiation defined by microscopy and quantitative proteomics in maize. Plant Cell **22:** 3509–3542

Martins MCM, Hejazi M, Fettke J, Steup M, Feil R, Krause U, Arrivault S, Vosloh D, Figueroa CM, Ivakov A, et al (2013) Feedback inhibition of starch degradation in Arabidopsis leaves mediated by trehalose 6-phosphate. Plant Physiol **163:** 1142–1163

Meiri A, Silk WK, Läuchli A (1992) Growth and deposition of inorganic nutrient elements in developing leaves of Zea mays L. Plant Physiol **99:** 972–978

Melo-Oliveira R, Oliveira IC, Coruzzi GM (1996) Arabidopsis mutant analysis and gene regulation define a nonredundant role for glutamate dehydrogenase in nitrogen assimilation. Proc Natl Acad Sci USA **93:** 4718–4723

Meyer S, Lauterbach C, Niedermeier M, Barth I, Sjolund RD, Sauer N (2004) Wounding enhances expression of AtSUC3, a sucrose transporter from Arabidopsis sieve elements and sink tissues. Plant Physiol **134:** 684–693

Miyashita Y, Good AG (2008) NAD(H)-dependent glutamate dehydrogenase is essential for the survival of Arabidopsis thaliana during dark-induced carbon starvation. J Exp Bot **59:** 667–680

Moore B, Zhou L, Rolland F, Hall Q, Cheng WH, Liu YX, Hwang I, Jones T, Sheen J (2003) Role of the Arabidopsis glucose sensor HXK1 in nutrient, light, and hormonal signaling. Science **300:** 332–336

Motose H, Takatani S, Ikeda T, Takahashi T (2012) NIMA-related kinases regulate directional cell growth and organ development through microtubule function in Arabidopsis thaliana. Plant Signal Behav **7:** 1552–1555

Nelissen H, Rymen B, Coppens F, Dhondt S, Fiorani F, Beemster GT (2013) Kinematic analysis of cell division in leaves of mono- and dicotyledonous species: a basis for understanding growth and developing refined molecular sampling strategies. Methods Mol Biol **959:** 247–264

Nelissen H, Rymen B, Jikumaru Y, Demuynck K, Van Lijsebettens M, Kamiya Y, Inzé D, Beemster GT (2012) A local maximum in gibberellin levels regulates maize leaf growth by spatial control of cell division. Curr Biol **22:** 1183–1187

O'Hara LE, Paul MJ, Wingler A (2013) How do sugars regulate plant growth and development? New insight into the role of trehalose-6-phosphate. Mol Plant **6:** 261–274

Osuna D, Usadel B, Morcuende R, Gibon Y, Bläsing OE, Höhne M, Günter M, Kamlage B, Trethewey R, Scheible WR, et al (2007) Temporal responses of transcripts, enzyme activities and metabolites after adding sucrose to carbon-deprived Arabidopsis seedlings. Plant J **49:** 463–491

Otsuga D, DeGuzman B, Prigge MJ, Drews GN, Clark SE (2001) REVOLUTA regulates meristem initiation at lateral positions. Plant J **25:** 223–236

Pal SK, Liput M, Piques M, Ishihara H, Obata T, Martins MCM, Sulpice R, van Dongen JT, Fernie AR, Yadav UP, et al (2013) Diurnal changes of polysome loading track sucrose content in the rosette of wildtype Arabidopsis and the starchless pgm mutant. Plant Physiol **162:** 1246–1265

Paul MJ, Primavesi LF, Jhurreea D, Zhang Y (2008) Trehalose metabolism and signaling. Annu Rev Plant Biol **59:** 417–441

Penning De Vries FWT (1975) Use of assimilates in higher plants. *In* JP Cooper, ed, Photosynthesis and Productivity in Different Environments. Cambridge University Press, New York, pp 457–480

Pick TR, Bräutigam A, Schlüter U, Denton AK, Colmsee C, Scholz U, Fahnenstich H, Pieruschka R, Rascher U, Sonnewald U, et al (2011) Systems analysis of a maize leaf developmental gradient redefines the current C4 model and provides candidates for regulation. Plant Cell **23:** 4208–4220

Pilkington SM, Encke B, Krohn N, Höhne M, Stitt M, Pyl ET (2015) Relationship between starch degradation and carbon demand for maintenance and growth in Arabidopsis thaliana in different irradiance and temperature regimes. Plant Cell Environ **38:** 157–171

Piques M, Schulze WX, Höhne M, Usadel B, Gibon Y, Rohwer J, Stitt M (2009) Ribosome and transcript copy numbers, polysome occupancy and enzyme dynamics in Arabidopsis. Mol Syst Biol **5:** 314

Poiré R, Wiese-Klinkenberg A, Parent B, Mielewczik M, Schurr U, Tardieu F, Walter A (2010) Diel time-courses of leaf growth in monocot and dicot species: endogenous rhythms and temperature effects. J Exp Bot **61:** 1751–1759

Pollock C, Farrar J, Tomos D, Gallagher J, Lu C, Koroleva O (2003) Balancing supply and demand: the spatial regulation of carbon metabolism in grass and cereal leaves. J Exp Bot **54:** 489–494

Price J, Laxmi A, St Martin SK, Jang JC (2004) Global transcription profiling reveals multiple sugar signal transduction mechanisms in Arabidopsis. Plant Cell **16:** 2128–2150

R Development Core Team (2011) R: A Language and Environment for Statistical Computing. R Foundation for Statistical Computing, Vienna, Austria

Rudra D, Warner JR (2004) What better measure than ribosome synthesis? Genes Dev **18:** 2431–2436

Running MP, Lavy M, Sternberg H, Galichet A, Gruissem W, Hake S, Ori N, Yalovsky S (2004) Enlarged meristems and delayed growth in plp mutants result from lack of CaaX prenyltransferases. Proc Natl Acad Sci USA **101:** 7815–7820

Rymen B, Coppens F, Dhondt S, Fiorani F, Beemster GT (2010) Kinematic analysis of cell division and expansion. Methods Mol Biol **655:** 203–227

Saeed AI, Sharov V, White J, Li J, Liang W, Bhagabati N, Braisted J, Klapa M, Currier T, Thiagarajan M, et al (2003) TM4: a free, open-source system for microarray data management and analysis. Biotechniques **34:** 374–378

Schindelin J, Arganda-Carreras I, Frise E, Kaynig V, Longair M, Pietzsch T, Preibisch S, Rueden C, Saalfeld S, Schmid B, et al (2012) Fiji: an open-source platform for biological-image analysis. Nat Methods **9:** 676–682

Schluepmann H, Pellny T, van Dijken A, Smeekens S, Paul M (2003) Trehalose 6-phosphate is indispensable for carbohydrate utilization and growth in Arabidopsis thaliana. Proc Natl Acad Sci USA **100:** 6849–6854

Schnable PS, Ware D, Fulton RS, Stein JC, Wei F, Pasternak S, Liang C, Zhang J, Fulton L, Graves TA, et al (2009) The B73 maize genome: complexity, diversity, and dynamics. Science **326:** 1112–1115

Scialdone A, Mugford ST, Feike D, Skeffington A, Borrill P, Graf A, Smith AM, Howard M (2013) Arabidopsis plants perform arithmetic division to prevent starvation at night. eLife **2:** e00669

Sheen J (2014) Master regulators in plant glucose signaling networks. J Plant Biol **57:** 67–79

Smeekens S, Ma J, Hanson J, Rolland F (2010) Sugar signals and molecular networks controlling plant growth. Curr Opin Plant Biol **13:** 274–279

Smith AM, Stitt M (2007) Coordination of carbon supply and plant growth. Plant Cell Environ **30:** 1126–1149

Stitt M (2013) Systems-integration of plant metabolism: means, motive and opportunity. Curr Opin Plant Biol **16:** 381–388

Stitt M, Heldt HW (1985) Generation and maintenance of concentration gradients between the mesophyll and bundle sheath in maize leaves. Biochim Biophys Acta **808:** 400–414

Stitt M, Zeeman SC (2012) Starch turnover: pathways, regulation and role in growth. Curr Opin Plant Biol **15:** 282–292

Sulpice R, Flis A, Ivakov AA, Apelt F, Krohn N, Encke B, Abel C, Feil R, Lunn JE, Stitt M (2014) Arabidopsis coordinates the diurnal regulation of carbon allocation and growth across a wide range of photoperiods. Mol Plant **7:** 137–155

Sulpice R, Trenkamp S, Steinfath M, Usadel B, Gibon Y, Witucka-Wall H, Pyl ET, Tschoep H, Steinhauser MC, Guenther M, et al (2010) Network analysis of enzyme activities and metabolite levels and their relationship to biomass in a large panel of Arabidopsis accessions. Plant Cell **22:** 2872–2893

Sweetlove LJ, Fernie AR (2013) The spatial organization of metabolism within the plant cell. Annu Rev Plant Biol **64:** 723–746

Sylvester AW, Cande WZ, Freeling M (1990) Division and differentiation during normal and liguleless-1 maize leaf development. Development **110:** 985–1000

Tang AC, Boyer JS (2008) Xylem tension affects growth-induced water potential and daily elongation of maize leaves. J Exp Bot **59:** 753–764

Thalor SK, Berberich T, Lee SS, Yang SH, Zhu X, Imai R, Takahashi Y, Kusano T (2012) Deregulation of sucrose-controlled translation of a bZIP-type transcription factor results in sucrose accumulation in leaves. PLoS One **7:** e33111

Thimm O, Bläsing O, Gibon Y, Nagel A, Meyer S, Krüger P, Selbig J, Müller LA, Rhee SY, Stitt M (2004) MAPMAN: a user-driven tool to display genomics data sets onto diagrams of metabolic pathways and other biological processes. Plant J **37:** 914–939

Tiessen A, Padilla-Chacon D (2013) Subcellular compartmentation of sugar signaling: links among carbon cellular status, route of sucrolysis, sink-source allocation, and metabolic partitioning. Front Plant Sci **3:** 306

Tohge T, Ramos MS, Nunes-Nesi A, Mutwil M, Giavalisco P, Steinhauser D, Schellenberg M, Willmitzer L, Persson S, Martinoia E, et al (2011) Toward the storage metabolome: profiling the barley vacuole. Plant Physiol **157:** 1469–1482

Usadel B, Bläsing OE, Gibon Y, Retzlaff K, Höhne M, Günther M, Stitt M (2008) Global transcript levels respond to small changes of the carbon status during progressive exhaustion of carbohydrates in Arabidopsis rosettes. Plant Physiol **146:** 1834–1861

Usadel B, Nagel A, Steinhauser D, Gibon Y, Bläsing OE, Redestig H, Sreenivasulu N, Krall L, Hannah MA, Poree F, et al (2006) PageMan: an interactive ontology tool to generate, display, and annotate overview graphs for profiling experiments. BMC Bioinformatics **7:** 535

Usadel B, Poree F, Nagel A, Lohse M, Czedik-Eysenberg A, Stitt M (2009) A guide to using MapMan to visualize and compare Omics data in plants: a case study in the crop species, Maize. Plant Cell Environ **32:** 1211–1229

Wahl V, Ponnu J, Schlereth A, Arrivault S, Langenecker T, Franke A, Feil R, Lunn JE, Stitt M, Schmid M (2013) Regulation of flowering by trehalose-6-phosphate signaling in Arabidopsis thaliana. Science **339:** 704–707 Wand MP, Jones MC (1995) Kernel Smoothing. Chapman and Hall, New York

Wang L, Czedik-Eysenberg A, Mertz RA, Si Y, Tohge T, Nunes-Nesi A, Arrivault S, Dedow LK, Bryant DW, Zhou W, et al (2014) Comparative analyses of C_4 and C_3 photosynthesis in developing leaves of maize and rice. Nat Biotechnol **32:** 1158–1165

Warner JR (1999) The economics of ribosome biosynthesis in yeast. Trends Biochem Sci **24:** 437–440

Weise SE, van Wijk KJ, Sharkey TD (2011) The role of transitory starch in C(3), CAM, and C(4) metabolism and opportunities for engineering leaf starch accumulation. J Exp Bot **62:** 3109–3118

Wiese A, Christ MM, Virnich O, Schurr U, Walter A (2007) Spatio-temporal leaf growth patterns of Arabidopsis thaliana and evidence for sugar control of the diel leaf growth cycle. New Phytol **174:** 752–761

Wiese A, Elzinga N, Wobbes B, Smeekens S (2005) Sucrose-induced translational repression of plant bZIP-type transcription factors. Biochem Soc Trans **33:** 272–275

Xiong Y, McCormack M, Li L, Hall Q, Xiang C, Sheen J (2013) Glucose-TOR signalling reprograms the transcriptome and activates meristems. Nature **496:** 181–186

Xiong Y, Sheen J (2014) The role of target of rapamycin signaling networks in plant growth and metabolism. Plant Physiol **164:** 499–512

Yadav UP, Ivakov A, Feil R, Duan GY, Walther D, Giavalisco P, Piques M, Carillo P, Hubberten HM, Stitt M, et al (2014) The sucrose-trehalose 6-phosphate (Tre6P) nexus: specificity and mechanisms of sucrose signalling by Tre6P. J Exp Bot **65:** 1051–1068

Yan J, Zhang C, Gu M, Bai Z, Zhang W, Qi T, Cheng Z, Peng W, Luo H, Nan F, et al (2009) The Arabidopsis CORONATINE INSENSITIVE1 protein is a jasmonate receptor. Plant Cell **21:** 2220–2236

Yazdanbakhsh N, Sulpice R, Graf A, Stitt M, Fisahn J (2011) Circadian control of root elongation and C partitioning in Arabidopsis thaliana. Plant Cell Environ **34:** 877–894

Zeeman SC, Kossmann J, Smith AM (2010) Starch: its metabolism, evolution, and biotechnological modification in plants. Annu Rev Plant Biol **61:** 209–234

Zhang Y, Primavesi LF, Jhurreea D, Andralojc PJ, Mitchell RAC, Powers SJ, Schluepmann H, Delatte T, Wingler A, Paul MJ (2009) Inhibition of SNF1-related protein kinase1 activity and regulation of metabolic pathways by trehalose-6-phosphate. Plant Physiol **149:** 1860–1871

Zhou M-L, Zhang Q, Sun Z-M, Chen L-H, Liu B-X, Zhang K-X, Zhu X-M, Shao J-R, Tang Y-X, Wu Y-M (2013) Trehalose metabolism-related genes in maize. J Plant Growth Regul **33:** 256